nature reviews clean technology

https://doi.org/10.1038/s44359-025-00102-9

Review article

Check for updates

Ammonia as a renewable energy carrier from synthesis to utilization

Zuxin Wen[1], Bing Huang[2], Yaolin Wang[3], Ke Wang[2], Xin Tu[3] ✉, Pengfei Xie[2] ✉ & Xianbiao Fu[1] ✉

Abstract

Ammonia has potential to play a key role in large-scale, long-term storage and transport of renewable energy. Renewable energy generation, particularly from solar and wind sources, has increased substantially but faces challenges such as intermittency and decentralization. Energy storage technologies are vital for addressing these issues, with chemical energy storage, especially ammonia, offering long-term (weeks) and large-scale (10–1,000 MW) energy storage. In this Review, we explore the role of ammonia in the energy landscape, focusing on its synthesis and utilization. Ammonia has advantages over hydrogen, such as higher volumetric energy density (12.7 MJ l^{-1}) and simpler storage requirements (readily liquefied at ~10 bar or −33 °C). It can be synthesized using renewable electricity and later decomposed to release hydrogen or used directly in fuel cells, including direct-ammonia fuel cells, indirect-ammonia fuel cells and ammonia solid-oxide fuel cells. We show that although decentralized ammonia synthesis under mild conditions offers potential for localized, low-carbon production, it remains limited by high energy costs and scalability challenges, underscoring the need for breakthroughs in catalyst efficiency and system design. The successful integration of ammonia into renewable energy systems will require coordinated efforts across technology development, policy support and infrastructure expansion.

Sections

[1]Department of Materials Science and Engineering, National University of Singapore, Singapore, Singapore. [2]College of Chemical and Biological Engineering, Zhejiang University, Hangzhou, China. [3]Department of Electrical Engineering and Electronics, University of Liverpool, Liverpool, UK. ✉e-mail: xin.tu@liverpool.ac.uk; pfxie@zju.edu.cn; xbfu@nus.edu.sg

Key points

- Ammonia is a promising carbon-free energy carrier with high volumetric energy density and ease of storage, suitable for large-scale and long-duration renewable energy storage and transport.
- Mild-condition ammonia synthesis, including electrochemical, plasma-catalytic and tandem plasma-electrocatalytic routes, offers potential for decentralized and flexible production using renewable electricity.
- Metal-mediated electrochemical nitrogen reduction has demonstrated high selectivity and stability, but scaling to industrial current densities and lifetimes remains a key challenge.
- Plasma-based and tandem plasma-electrocatalytic approaches enable operation under ambient conditions and modular deployment, but energy efficiency and catalyst performance need further improvement.
- Ammonia can be decomposed to supply hydrogen for fuel cells or combustion, with ongoing efforts focused on lowering the reaction temperature and replacing costly ruthenium-based catalysts.
- Realizing cost-competitive, sustainable ammonia production and its full potential as a carbon-free energy carrier will require integrated advances in catalysts, reactors and system-level design, supported by policy and infrastructure to drive scalable deployment.

Introduction

Global annual renewable electricity generation reached 8,640 TWh in 2022, accounting for 30% of the total global electricity consumption[1]. Despite this progress, renewable energy sources, such as solar and wind power, still face inherent challenges such as fluctuation, intermittency and decentralized generation[2]. Addressing these challenges requires energy storage technologies that can bridge the gap between energy supply and demand. By capturing and storing energy during periods of high production, storage systems can release energy during times of low generation, balancing supply and demand[3].

Storage scale and storage time are two crucial factors in evaluating energy storage technologies. Among different energy storage technologies, chemical energy storage provides large-scale and long-term energy storage[2] (Fig. 1a). Chemical energy carriers such as methane, methanol, hydrogen (H_2) and ammonia (NH_3) enable efficient energy storage and transport. However, owing to the carbon dioxide (CO_2) emissions from synthesis and utilization of methane and methanol, there is a growing focus on carbon-free alternatives.

Ammonia and hydrogen have emerged as leading candidates, with ammonia offering several advantages over hydrogen, particularly for large-scale storage and transportation applications[2,4–8]. For instance, liquid ammonia (12.7 MJ l^{-1}) offers a higher volumetric energy density than liquid hydrogen (8.5 MJ l^{-1}) (Fig. 1b). Moreover, ammonia remains in liquid form under moderate pressures and temperatures, simplifying the infrastructure requirements compared with hydrogen, which requires ultra-low temperatures or high pressures for storage. Hydrogen liquefies at −253 °C under 1 bar of pressure, whereas ammonia liquefies at −33 °C under 1 bar or at room temperature under 10 bar of pressure[4,5]. Furthermore, regardless of the transportation method, whether by ship or pipeline, the cost per kilogram of hydrogen when transported as ammonia is lower than that of pure hydrogen[9] (Fig. 1c). In terms of safety during handling and storage, ammonia has a high auto-ignition temperature, which can reduce the risk of accidental ignition[5]. However, to ensure optimal combustion, it might need to be mixed with other fuels that act as combustion promoters[10] (Fig. 1d). Moreover, ammonia is toxic, can produce NO_x emissions during combustion, and presents challenges in catalytic decomposition such as sluggish kinetics at low temperatures and catalyst deactivation due to nitrogen poisoning[4,8].

With rapid advancements in renewable energy technologies and the increasing need for large-scale energy storage solutions, reassessing ammonia's role in the energy landscape is timely[9]. Ammonia synthesis under ambient conditions (25 °C and 1 atm), catalyst design for ammonia decomposition and ammonia utilization in energy conversion systems have improved the feasibility of ammonia-based energy systems[11,12]. In particular, distributed ammonia synthesis methods, such as metal-mediated electrochemical ammonia synthesis, direct plasma-catalytic ammonia synthesis and tandem plasma-electrocatalytic processes[13–15], have shown notable variations in ammonia production rates and energy costs. These differences highlight trade-offs between efficiency, scalability and practical deployment.

In this Review, we examine ammonia synthesis processes and ammonia decomposition and utilization strategies. We discuss ammonia synthesis using renewable electricity (that is, power-to-ammonia, charging), emphasizing energy cost, sustainability and industrial scalability. Furthermore, we explore ammonia decomposition for hydrogen production (ammonia-to-hydrogen), emphasizing catalyst design and mechanisms to enhance reaction efficiency. Finally, we assess ammonia's role in energy conversion technologies (that is, ammonia-to-power, discharging), with a particular focus on ammonia fuel cells. We discuss different fuel cell types, including direct-ammonia fuel cells, indirect-ammonia fuel cells and ammonia-fed solid-oxide fuel cells (SOFCs), analysing their performance, mechanisms and challenges such as ammonia crossover, catalyst degradation and fuel purification requirements.

Ammonia as an energy carrier

Ammonia can act as an energy carrier, with different roles in renewable energy storage and conversion[4–6] (Fig. 2). Energy generated from renewable sources such as solar, wind, hydropower and ocean wave power[16] can be utilized to power air separation and water electrolysis, which provide nitrogen and hydrogen feedstocks, respectively. In addition, renewable electricity can directly drive the electrochemical ammonia synthesis from these inputs, enabling a fully renewable ammonia production pathway.

The main challenge of using ammonia as an energy carrier in decarbonized energy systems lies in developing efficient and clean ammonia synthesis technologies powered by decentralized renewable energy[11,12,17]. Once synthesized, ammonia can be efficiently stored and transported, leveraging existing infrastructure[6]. For utilization, ammonia can be converted back into power through different means, including power generation plants, vehicle and marine fuels, and ammonia fuel cells[5]. Additionally, ammonia can be decomposed to produce hydrogen, which can be further used in fuel cells and ammonia combustion promoters[7].

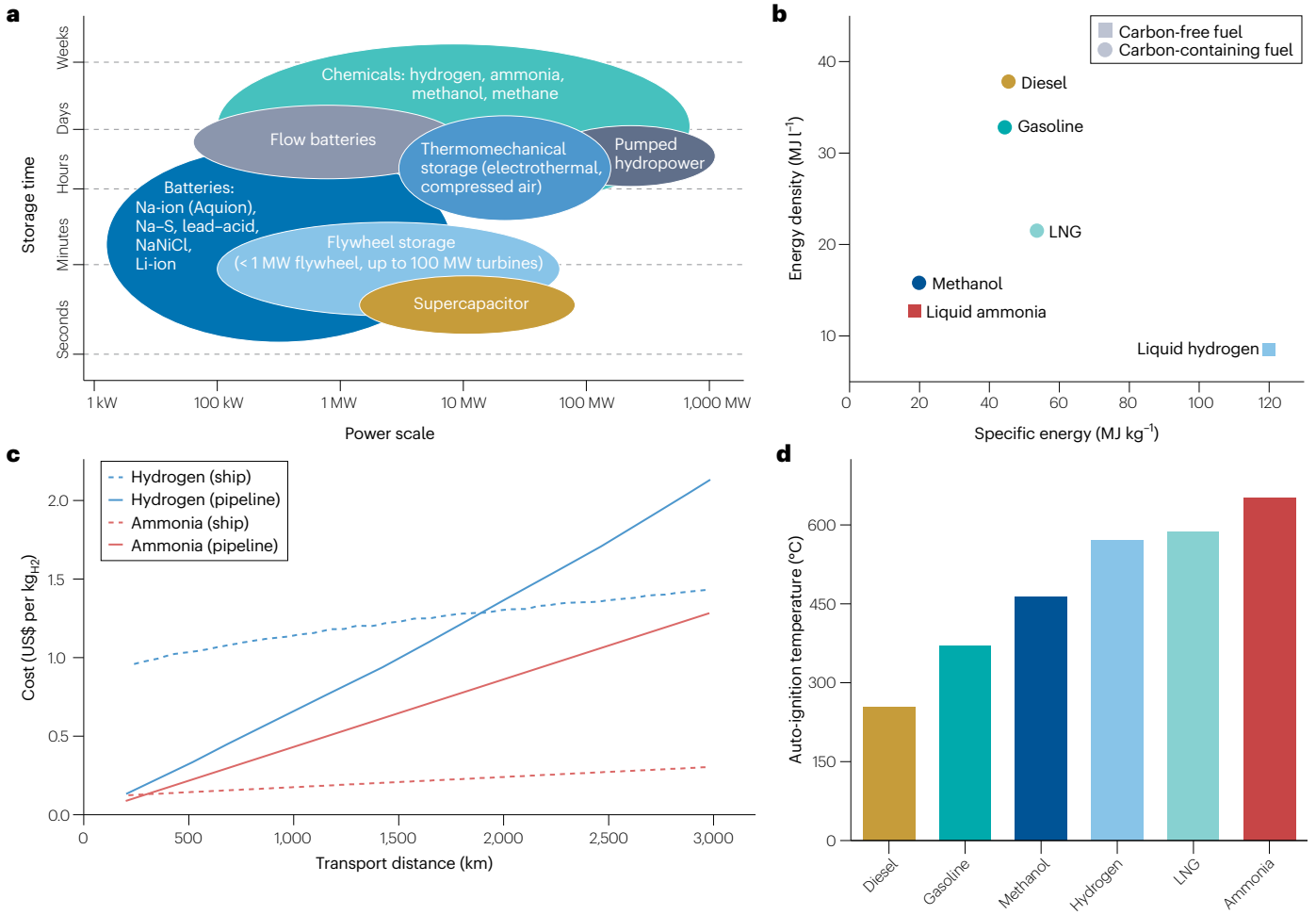

Fig. 1 | Energy storage technologies and the role of ammonia as an energy carrier. a, Among various energy storage technologies, chemical energy storage stands out for long-term and large-scale applications[2]. **b**, Carbon-free fuels and carbon-containing fuels provide high energy density and specific energy, whereas ammonia (NH_3) offers a higher volumetric energy density than liquid hydrogen[5]. **c**, Ammonia has a lower transport cost per unit of hydrogen (H_2), based on cost estimates for transport of energy by ship and pipeline[9]. **d**, Ammonia requires a higher temperature for ignition compared with conventional hydrocarbons and hydrogen[5]. LNG, liquefied natural gas. Data from ref. 5. Panel **a** adapted with permission from ref. 2, Elsevier. Panel **b** adapted with permission from ref. 5, Elsevier. Panel **c** adapted from ref. 9, CC BY 4.0.

Ammonia synthesis under mild conditions

Ammonia synthesis from renewable sources enables the capture and storage of intermittent energy from solar and wind power in a stable and transportable form. However, synthesizing ammonia economically and efficiently under mild conditions (temperature <150 °C and pressure <20 atm) remains challenging[12,17]. The main method for industrial ammonia production, the Haber–Bosch process, is highly energy-intensive, requiring high temperatures (350–450 °C) and pressures (150–200 atm)[12,18]. This process consumes about 1–2% of the world's energy supply and contributes to about 1.3% of global CO_2 emissions[16]. The Haber–Bosch process also requires a substantial capital investment due to its harsh reaction conditions, which tends to result in centralized ammonia production[19]. Ammonia is typically produced on a large scale at central facilities and then transported to various locations. Whereas the Haber–Bosch process is economically viable with centralized production, renewable energy sources are decentralized[20]. This mismatch makes it challenging to align the centralized Haber–Bosch process with the decentralized nature of renewable energy. Therefore, it is important to develop distributed ammonia production methods that are flexible, are cost-effective and operate under milder conditions to effectively store decentralized renewable energy.

Substantial efforts have been invested in exploring alternative methods for ammonia synthesis under milder or ambient conditions, such as enzyme catalysis, homogeneous catalysis (for example, nitrogenase mimics), electrochemistry (for example, electrocatalysis), photocatalysis, plasma catalysis, chemical looping and mechanochemical synthesis[21–26]. Mechanochemical ammonia synthesis offers an alternative to thermally driven processes, enabling ammonia production at ambient pressure and near-room temperature via mechanical activation of nitrogen over metal catalysts through ball milling[26]. This section focuses on advances and challenges of three ammonia synthesis

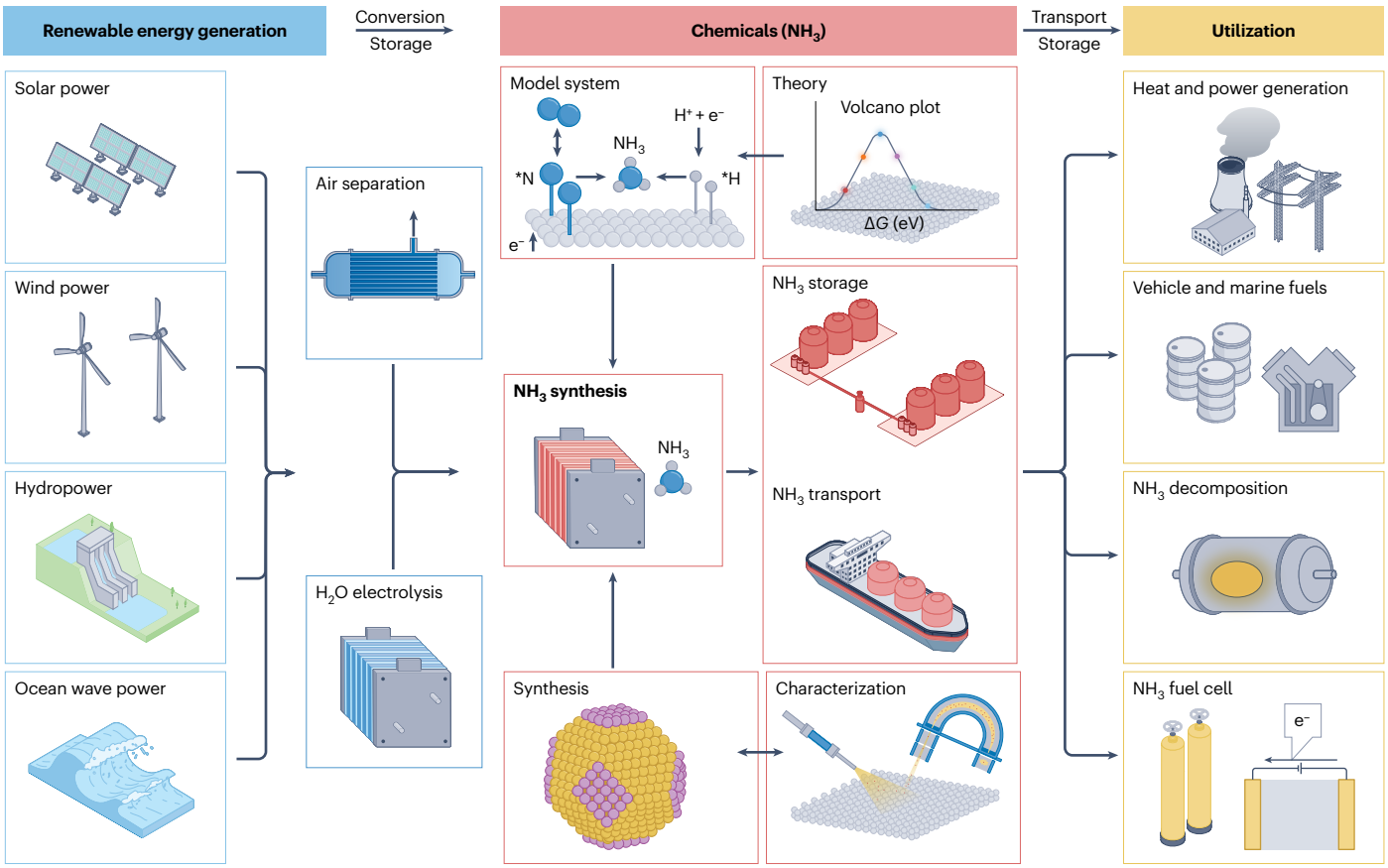

Fig. 2 | Ammonia as an energy carrier in energy storage and conversion. Ammonia (NH_3) is emerging as a key contributor to the decarbonization of energy systems, from renewable energy-driven synthesis and scalable storage solutions to its use in combustion, fuel cells and catalytic hydrogen (H_2) extraction. In routes involving hydrogen input (for example, lithium or calcium-mediated or plasma-assisted nitrogen reduction reaction (NRR)), electrolysis-derived hydrogen must be purified and dried prior to use to avoid moisture-induced side reactions or plasma destabilization. Catalyst and process development across the entire ammonia-based energy systems chain is supported by fundamental scientific foundations, model systems, theory, synthesis and characterization. The asterisk represents a vacant active site on the catalyst surface.

technologies under milder or ambient conditions: metal-mediated electrochemical ammonia synthesis; direct plasma-catalytic ammonia synthesis from nitrogen (N_2) and hydrogen; and a two-step process of plasma-catalytic conversion and electrochemical reduction (Fig. 3).

Metal-mediated electrochemical ammonia synthesis

The metal-mediated nitrogen reduction reaction (M-NRR), in non-aqueous electrolytes[24,27], uses lithium (Li-NRR) and calcium (Ca-NRR) as mediators[28–32]. In the M-NRR process, a metal ion (for example, Li^+ or Ca^{2+}) diffuses from the bulk electrolyte through the solid-electrolyte interphase (SEI) and is electrochemically reduced to its metallic form on the electrode[33–36] (Fig. 3a). The fresh metal then activates nitrogen to form surface metal-nitride intermediates, which are subsequently protonated by a proton shuttle (for example, ethanol) to release ammonia and metal ions[13,28,37]. The proton shuttle enables proton transfer from the anode (H_2 oxidation) to the cathode, protonating metal nitride (MN_xH_y) intermediates to facilitate ammonia formation[37,38]. The proton shuttle also helps to form a functional SEI layer on the cathode, which stabilizes the metal surface and improves reaction efficiency[38–40].

The NH_3 production rates vary substantially across different experimental studies of metal-mediated ammonia synthesis processes[19,29,31,35,36,41–44] (Fig. 3d and Supplementary Table 1). A geometric current density of -1 A cm^{-2} was achieved in a pressurized batch-type reactor (20 bar) using high surface-area electrodes, resulting in an ammonia production rate of 2,600 nmol cm^{-2} s^{-1} (ref. 35) (Fig. 3d). Additionally, nearly 100% Faradaic efficiency (FE) for ammonia was achieved using lithium bis(trifluoromethanesulfonyl)imide (LiTFSI) in a pressurized batch reactor (15 bar), with an ammonia production rate of 150 nmol cm^{-2} s^{-1} (ref. 36). In both instances, a sacrificial organic solvent was used as the proton donor.

Water can also be directly employed as a proton source in lithium-mediated systems by constructing a biphasic hybrid electrolyte configuration. In such a system, an aqueous anolyte and an organic catholyte are separated by an anion exchange membrane (AEM), and enable stable NH_3 production with ~60% FE for up to 50 h under a current density of -5 mA cm^{-2}. This approach also mitigates solvent degradation by using an aqueous anolyte at the anode, ensuring that water, rather than the organic solvent, undergoes oxidation[45]. A major challenge in hybrid electrolyte systems is water crossover from

the aqueous anolyte to the organic catholyte, which elevates water content, disrupts lithium deposition and promotes the formation of insulating lithium oxide and hydroxide layers. Water crossover limits stable operation to ~50 h, and highlights the need for effective water management strategies to suppress cross-phase transport and enable longer-term stability[45].

In flow reactors, the hydrogen oxidation reaction (HOR), at the anode side, can be used as a proton source, at ambient pressure and temperature[29], with FE of 60–70%, energy efficiency of 13–17%, a current density of −6 mA cm^{-2} and a minimum lifetime of 300 h (refs. 29,38,42). Under short-term operation (a few minutes), a current density of −60 mA cm^{-2} (ref. 42) and an ammonia production rate of 30 nmol cm^{-2} s^{-1} can be achieved when coupled with the HOR[32]. An ammonia production rate of 10.2 nmol cm^{-2} s^{-1} sustained over 300 h can be achieved, with approximately 98% of the produced ammonia present in the gas phase when using flow reactors. Such a gas phase-dominant product distribution substantially reduces the cost and complexity associated with ammonia separation[42]. If the produced ammonia remains dissolved in the reaction medium, a dedicated separation step becomes necessary, typically involving techniques such as air stripping, membrane distillation, gas-permeable membranes, electrodialysis and ion exchange[46].

To bring the ammonia concentration within the range required for feasibility and scalability of separation (typically >10,000 mg_N l^{-1}), strategies such as prolonging the electrolysis time, increasing the current density or applying electrochemical ammonia accumulation can be employed[47]. Electrochemical separation strategies, particularly gas diffusion electrode-based membrane stripping, have energy inputs as low as 7.4 kWh per kg_N at initial ammonia concentrations of 2,500–3,000 mg_N l^{-1} (ref. 48). Even at lower concentrations around 748 mg_N l^{-1}, electrochemical membrane stripping and hybrid recovery approaches show comparable efficiencies (~7 kWh per kg_N) under ambient conditions[49].

Based on the performance of existing industrial processes, such as the chlor-alkali industry, which typically operates at current densities of 200–400 mA cm^{-2}, a similar or higher range of current density would be required for industrial-scale electrochemical ammonia production[14]. Achieving high current densities in continuous-flow reactors with the HOR, such as those exceeding 200 mA cm^{-2}, along with FE greater than 90%, remains a challenge for the industrial-scale application of metal-mediated ammonia synthesis[37]. Developing high surface-area gas diffusion electrodes and optimizing reactor engineering are potential approaches to achieving high current densities in electrochemical ammonia synthesis. For electrochemical ammonia synthesis to be industrially viable, the process needs to demonstrate stable performance for at least several months to years, matching the stability benchmarks set by established industrial processes such as chlor-alkali production[50]. More importantly, the electrochemical ammonia synthesis system needs to adapt to fluctuating energy inputs, a requirement that has not yet been experimentally validated.

Direct plasma-catalytic ammonia synthesis

Non-thermal plasma generates a mixture of energetic electrons and reactive species capable of activating N_2 and initiating chemical reactions under ambient conditions (Fig. 3b). The combination of non-thermal plasma with catalysis offers advantages such as enhanced reaction rates, selectivity and energy efficiency[51]. Plasma-induced vibrationally excited N_2 can effectively lower the dissociative adsorption energy barrier of N_2 molecules on nickel and cobalt nanoparticles, which exhibit weak nitrogen binding and are not active in thermal catalysis, enabling catalytic NH_3 synthesis on nickel and cobalt nanoparticles under ambient plasma conditions[25]. Reducing the N_2 dissociation barrier might help to expand catalyst options beyond iron-based materials, which are commonly used in the Haber–Bosch process[25,52].

However, achieving high ammonia yields (>6%) while maintaining low energy costs (<100 GJ per $tonne_{NH3}$) remains a challenge, as both metrics are strongly governed by catalyst performance. Balancing ammonia yield with energy efficiency ultimately depends on how catalysts mediate nitrogen activation and energy transfer. A low energy cost of 163.9 GJ per $tonne_{NH3}$ was obtained using a Ru–Mg–Al_2O_3 catalyst, but the ammonia yield was only 0.105%[53]. A higher ammonia yield of 6.4% was achieved with a Ni–SiO_2–$BaTiO_3$ catalyst, but at a substantially higher energy cost of 6,283.0 GJ per $tonne_{NH3}$ (ref. 54) (Fig. 3d). One possible strategy to overcome this trade-off between yield and energy cost is adsorption-enhanced plasma catalysis[15,55]. By using porous material-based catalysts, ammonia can diffuse into the pores of the catalyst, owing to the gradient in ammonia concentration inside and outside the pores[15]. Plasma typically cannot be generated in such small pores (nanometres), reducing ammonia decomposition induced by the plasma and shifting the reaction equilibrium[15]. This approach has been demonstrated successfully using different porous materials, including MCM-41, zeolites and $MgCl_2$ (refs. 15,55,56).

To advance plasma-catalytic ammonia synthesis, focus should be on the rational design of catalysts that incorporate sorption enhancement strategies to increase ammonia yields and energy efficiency[57].

Tandem plasma-electrocatalytic ammonia synthesis

The integration of non-thermal plasma and electrocatalysis involves the plasma oxidation of nitrogen into high-concentration NO_x (NO and NO_2), followed by the electrocatalytic reduction of NO^{y-}_x (NO, N_2O, NO_2, NO_3^-, NO_2^-) to ammonia (Fig. 3c). This tandem process leverages the strengths of both plasma technology and electrocatalysis, potentially enabling ammonia production from readily available resources such as air and water using renewable energy. Non-thermal plasma systems consume energy of approximately 123.9 GJ per $tonne_{NOx}$ for a reasonable NO_x yield (for example, >1%)[58]. Moreover, through optimal electrocatalyst design, the energy cost for NH_3 production via the NO reduction reaction can be reduced to 67.1 GJ per $tonne_{NH3}$ (ref. 59), bringing the overall energy cost of the tandem process to a competitive level of 344.6 GJ per $tonne_{NH3}$.

Using a tandem non-thermal plasma-electrocatalysis approach, a system combining spark discharge plasma and a Ni$(OH)_x$–Cu catalyst demonstrated a remarkable ammonia yield rate of 3 mmol h^{-1} cm^{-2} and FE of 92%[60]. Moreover, a $La_{1.5}Sr_{0.5}Ni_{0.5}Fe_{0.5}O_4$ perovskite oxide has been employed as a catalyst for the NO_x reduction reaction under acidic conditions (pH 0), achieving almost 100% FE for ammonia and an ammonia yield of 2,375 nmol cm^{-2} s^{-1} at a current density of −2 A cm^{-2} (ref. 61) (Fig. 3d). Remarkably, this catalyst maintains a stable cell voltage and FE for more than 350 h under industrially relevant current densities in a membrane electrode assembly configuration. By stacking multiple membrane electrode assemblies in series, an ammonia production rate of 2.6 g h^{-1} was achieved at 20 A[61]. Techno-economic and life-cycle assessments show that this system offers a more cost-effective ammonia production pathway compared with the Haber–Bosch process, especially when electricity costs are below US$22 MWh^{-1} (ref. 61).

To optimize energy efficiency and NH_3 yield, it is important to design catalysts that selectively reduce NO_x to ammonia while minimizing competing side reactions[62,63]. Efficient ammonia separation from

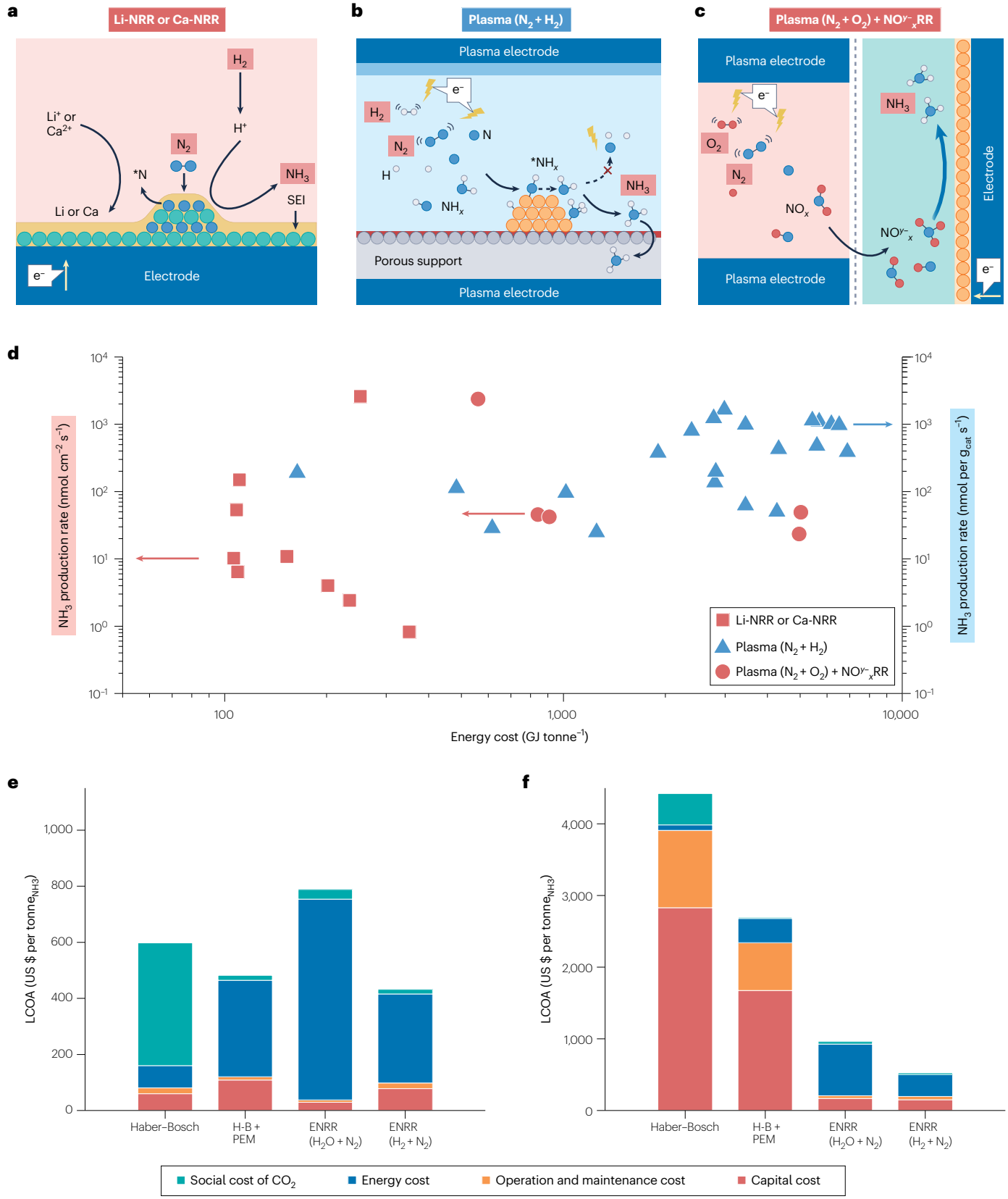
a
Li-NRR or Ca-NRR
H2
Li+ or Ca2+
H+
N2
*N
NH3
SEI
Li or Ca
e−
Electrode
b
Plasma (N2 + H2)
Plasma electrode
e−
H2
N2
N
H
*NHx
NHx
NH3
Porous support
Plasma electrode
c
Plasma (N2 + O2) + NOy−x RR
Plasma electrode
e−
O2
N2
NOx
NH3
NOy−x
Electrode
Plasma electrode
e−
d
NH3 production rate (nmol cm−2 s−1)
NH3 production rate (nmol per gcat s−1)
Energy cost (GJ tonne−1)
100
1,000
10,000
Li-NRR or Ca-NRR
Plasma (N2 + H2)
Plasma (N2 + O2) + NOy−x RR
e
LCOA (US $ per tonneNH3)
Haber–Bosch
H-B + PEM
ENRR (H2O + N2)
ENRR (H2 + N2)
f
LCOA (US $ per tonneNH3)
Haber–Bosch
H-B + PEM
ENRR (H2O + N2)
ENRR (H2 + N2)
Social cost of CO2
Energy cost
Operation and maintenance cost
Capital cost

Fig. 3 | Ammonia synthesis under mild conditions. a, Metal-mediated electrochemical ammonia (NH_3) synthesis. In a lithium or calcium-mediated nitrogen reduction reaction (Li-NRR or Ca-NRR) process, Li^+ or Ca^{2+} ions diffuse through the solid-electrolyte interphase (SEI), are reduced to metal at the cathode and activate nitrogen to form lithium or calcium nitride intermediates, which are subsequently protonated to release ammonia. **b**, Direct plasma-catalytic ammonia synthesis from nitrogen (N_2) and hydrogen (H_2). Non-thermal plasma generates energetic electrons and vibrationally excited nitrogen molecules in plasma-assisted ammonia synthesis, enhancing the catalytic activation of nitrogen and facilitating ammonia formation under mild conditions. Plasma electrode refers to plasma-assisted systems operating at voltages typically in the 10–25 kV range. **c**, Tandem plasma-electrocatalytic ammonia synthesis. Two-step ammonia synthesis combines plasma oxidation of nitrogen to NO^{y-}_x (NO, N_2O, NO_2, NO_3^-, NO_2^-) species followed by electrochemical reduction of NO^{y-}_x to ammonia, leveraging the advantages of plasma activation and electrocatalytic selectivity. **d**, Energy cost and ammonia production rate of lithium or calcium-mediated electrochemical, direct plasma-catalytic and tandem plasma-electrocatalytic ammonia synthesis routes under milder conditions. The data used in the figure are from refs. 15,19,29,31,35,36,41–44,53,61,75,76,149–154 and are provided in Supplementary Table 1. **e**, Levelized cost of ammonia (LCOA) for different ammonia synthesis technologies at a production scale of 2,000 $tonnes_{NH3}$ per day. **f**, LCOA for different ammonia synthesis technologies at a production scale of 30 kg_{NH3} per day. The asterisk represents a vacant active site on the catalyst surface. ENRR (H_2 + N_2), electrochemical nitrogen reduction reaction with H_2 and N_2 as reactants; ENRR (H_2O + N_2), electrochemical nitrogen reduction reaction with H_2O and N_2 as reactants; H-B + PEM, Haber–Bosch and H_2 from proton-exchange membrane electrolysis; NO^{y-}_xRR, electrochemical NO^{y-}_x reduction reaction. Panels **e** and **f** adapted with permission from ref. 78, CC BY 4.0.

the product stream is also essential for overall process economics. Integrating the plasma reactor, electrolyser and ammonia separation unit into a compact and modular system might facilitate commercialization by reducing capital and operating costs, enabling shared utility infrastructure and supporting small-scale distributed deployment[60].

Scalability and economics

The large-scale implementation of ammonia as a renewable energy carrier depends on the energy cost, technology readiness, economic feasibility and environmental sustainability of its production[64]. Although ammonia has shown promise as a zero-carbon energy carrier, the challenges associated with its production must be thoroughly assessed to ensure its viability in future energy systems.

Energy cost. The energy cost of a process, which refers to the amount of energy required to produce a specific quantity of output, is a crucial parameter for evaluating the potential applicability of technology[64]. The Haber–Bosch process has been continuously optimized in terms of energy efficiency, reducing the minimum energy cost from more than 60 GJ per $tonne_{NH3}$ in the mid-1950s to the current best available technology level of around 30 GJ per $tonne_{NH3}$ when using natural gas via steam reforming[64,65]. By contrast, for plants based on coal gasification through partial oxidation, the energy cost of the overall Haber–Bosch process is approximately 166 GJ per $tonne_{NH3}$ (ref. 65). Coal gasification through partial oxidation converts coal into syngas (CO and H_2), providing hydrogen for the Haber–Bosch process after CO removal via water–gas shift and CO_2 scrubbing[66].

For metal-mediated electrochemical ammonia synthesis, theoretical energy costs, assuming 100% FE and no overpotential, are 51.8 GJ per $tonne_{NH3}$ for Li-NRR and 48.8 GJ per $tonne_{NH3}$ for Ca-NRR[67]. Experimentally, the energy cost for metal-mediated electrochemical ammonia synthesis is approximately 110 GJ per $tonne_{NH3}$ (Fig. 3d), based on a continuous-flow system using the HOR as the proton source under ambient conditions[29]. The higher experimental value arises from kinetic overpotentials, ohmic resistance and side reactions that lower the overall energy efficiency under practical conditions. This value (110 GJ per $tonne_{NH3}$) is regarded as a representative benchmark for current performance assessment and future improvement[67]. For comparison with the theoretical value, an energy consumption as low as 64 GJ per $tonne_{NH3}$ has been achieved using a lithium-mediated approach based on a system employing a lithium-ion conducting glass ceramic electrolyte, highlighting the potential for further energy optimization in well-controlled experimental setups[68]. Economically and energetically competitive operation requires mediators with less negative reduction potentials, along with catalyst and reactor designs that maintain low overpotentials without compromising selectivity[14]. As a performance target, electrochemical processes should aim for energy efficiency above 86% and ammonia production rates exceeding 7×10^{-7} mol cm^{-2} s^{-1}, at current densities greater than 300 mA cm^{-2} and 90% FE[40].

For plasma-catalytic NH_3 synthesis from N_2 and H_2, the lowest theoretical energy cost is 1.6 GJ per $tonne_{NH3}$, based on the minimum energy requirement for vibrational excitation of N_2 (Fig. 3d). Assuming a 10% energy efficiency, the minimum theoretical energy cost is 16.0 GJ per $tonne_{NH3}$ (ref. 57). For the tandem plasma-electrocatalysis process, the minimum theoretical energy cost for plasma synthesis of NO_x is 3.2 GJ per $tonne_{NO}$ (ref. 57). Combined with the theoretical energy cost for the NO reduction reaction at 100% FE (23.6 GJ per $tonne_{NH3}$), the overall minimum theoretical energy cost for this tandem process is ~30.7 GJ per $tonne_{NH3}$. Controlling the NO:NO_2 ratio and enhancing NO_x solubility in the electrolyte are important for reducing energy costs within the tandem process[69,70].

Electrochemical ammonia synthesis and plasma-catalytic ammonia synthesis, by enabling decentralized and localized production, diminish reliance on centralized facilities and supply chains, thereby reducing transportation costs and aligning with the decentralized nature of renewable energy. This decentralization also mitigates dependence on specific regions, reducing vulnerability to geopolitical instabilities and enhancing the strategic desirability of these approaches, even if energy consumption is slightly higher[29].

Technology readiness level. The technology readiness level (TRL) framework provides a structured evaluation of a technology's development stage, from conceptual research (TRL 1–3) to pilot-scale validation (TRL 4–6) and full commercial deployment (TRL 7–9)[71]. Conventional Haber–Bosch ammonia synthesis is a mature technology (TRL 9), benefiting from decades of optimization, but its reliance on high temperatures (350–450 °C) and pressures (150–200 atm) limits flexibility[64]. By contrast, emerging on-site ammonia synthesis routes remain at early TRLs (TRL 1–4).

In metal-mediated electrochemical ammonia synthesis, lithium-mediated ammonia synthesis has reached a relatively high TRL of 4, with laboratory validation demonstrating ammonia production exceeding 4 g and an energy efficiency of 17%[72] (Table 1). Although

Table 1 | TRLs of ammonia synthesis-related technologies

Technologies related to ammonia synthesis	TRL	Refs.
Renewable energy generation	9	1
Air separation to produce nitrogen	9	64,78
Alkaline electrolysis for hydrogen production	9	64
Proton-exchange membrane electrolysis for hydrogen production	7–8	64
Metal-mediated electrochemical ammonia synthesis	1–4	29,42,79
Direct plasma-catalytic ammonia synthesis	1–3	15
Tandem plasma-electrocatalytic process	2–4	60,74

TRL, technology readiness level.

gram-scale production and 300 h of stable operation in a 25 cm^2 flow cell have been achieved, substantial challenges remain for scaling towards industrial deployment[42]. Transitioning from single-cell systems to stacked electrolysis cells requires improvements in electrode durability, electrolyte stability and reactant transport to maintain high efficiency under large-scale operation[14]. Future advancements should focus on scalable cell stack design for efficient reactant distribution and heat management, improved lithium recovery to reduce material loss and enhanced system integration to optimize electrolyte composition and electrode performance, ensuring industrial-scale feasibility with high efficiency and stability[17].

The direct plasma-catalytic ammonia synthesis process remains in its early development stage, with a TRL of 1–3. By optimizing plasma conditions and employing appropriate catalysts, such as ruthenium, cobalt or nickel-based catalysts, ammonia production can achieve gram-scale yields, ranging from 0.05 to 0.2 g h^{-1} (refs. 15,53,73). Furthermore, after more than 150 h of continuous discharge, Ni–MCM-41 has shown stable catalytic performance and consistent energy efficiency (2.1%)[15]. Laboratory-scale demonstrations have confirmed feasibility, but the absence of pilot-scale implementations limits its industrial readiness.

The tandem plasma-electrocatalytic process has a slightly higher TRL of 2–4, benefiting from advances in plasma-driven NO^{y-}_{x} synthesis and electrochemical NO^{y-}_{x} reduction reaction ($NO^{y-}_{x}RR$)[60]. In continuous-flow plasma-electrocatalytic systems, ammonia production rates of 1.6–5.1 g h^{-1} have been achieved[60,70,74,75], with stable operation for more than 1,000 h[70]. In this tandem process, primary energy consumption occurs in the NO^{y-}_{x} generation stage, accounting for 69–93% of the total energy usage, depending on the specific plasma type employed[76,77]. By contrast, the electrochemical NO^{y-}_{x} reduction step is relatively established[62]. Therefore, research efforts should focus on optimizing plasma-driven NO^{y-}_{x} production, including improving plasma energy efficiency, NO^{y-}_{x} selectivity and reaction kinetics, to enhance the overall system feasibility and economic viability. Additionally, further advancements in reactor design, NO^{y-}_{x} separation and catalyst stability are necessary to reduce operational costs and accelerate industrial scalability.

Techno-economics. The levelized cost of ammonia (LCOA) accounts for capital expenditures (CAPEX), operational and maintenance costs (OPEX), and energy costs, providing a comprehensive basis for assessing the economic feasibility of different ammonia production technologies[64,78]. It should be noted that the LCOA of ammonia production is influenced by the scale of production[78] (Fig. 3e,f). At production capacities of ~2,000 $tonne_{NH3}$ per day, the cost can be as low as US$159 per $tonne_{NH3}$, excluding the social cost of CO_2 emissions[78] (Fig. 3e). However, small-scale Haber–Bosch plants experience severe diseconomies of scale, with costs exceeding US$4,000 per $tonne_{NH3}$ when production is reduced to ~30 kg_{NH3} per day[78] (Fig. 3f). This sharp increase is primarily attributed to capital cost escalation, as small-scale facilities cannot fully leverage the high efficiency and heat integration that benefit large-scale operations[78].

The cost of ammonia for electrochemical nitrogen reduction reaction (ENRR) at a production scale of ~2,000 $tonne_{NH3}$ per day is estimated to be ~US$430 per $tonne_{NH3}$ when the social cost of CO_2 emissions is included, making it more competitive than the Haber–Bosch process (~US$600 per $tonne_{NH3}$)[78]. The choice between hydrogen-fed and water-fed anodic configurations involves trade-offs in system efficiency, integration complexity and operational cost[78] (Fig. 3e,f). Although the HOR enables lower overpotentials (~50 mV) and higher selectivity (>99%), it requires a purified H_2 supply (>99.99%) and gas handling infrastructure, which increases the complexity and cost of the system[29,32,78]. By contrast, water-fed systems based on the oxygen evolution reaction offer simpler integration with renewable sources, but suffer from higher cell voltages and reduced energy efficiency[78]. Techno-economic analyses have shown that hydrogen-fed systems can reach energy efficiencies of up to 28%, substantially outperforming the ~7% efficiency observed in water-fed electrochemical nitrogen reduction, although at the expense of added upstream energy input[78].

For lithium-mediated ammonia synthesis, the estimated LCOA is less than US$700 per $tonne_{NH3}$ at a production scale of ~154 $tonne_{NH3}$ per day[79]. Ammonia can be produced economically (below US$1,000 per $tonne_{NH3}$) at large scales (250 $tonne_{NH3}$ per day) if electrochemical reactors achieve partial ammonia currents above 400 mA cm^{-2}, energy efficiencies exceeding 30% and long-term operational stability over several years[80]. Despite promising achievements in selectivity (~70%) and 300 h stability in laboratory-scale flow cells, further advancements in reactor design, lithium recycling strategies, current density enhancement and long-term stability are essential[29,38,42]. Electrochemical ammonia synthesis can achieve near-zero carbon emissions when powered by renewable electricity[78]. However, its sustainability also relies on advancing closed-loop metal recovery systems to minimize resource depletion and replacing toxic or resource-intensive mediators[14]. Additionally, developing new mediators and high-performance catalysts could help to improve energy efficiency and scalability, ultimately achieving cost parity with the Haber–Bosch process[17].

Plasma-based ammonia synthesis faces economic challenges due to its low energy efficiency, which substantially increases the operating costs, particularly electricity expenses[57]. Plasma synthesis requires approximately 9.3 times more energy than the Haber–Bosch process to produce the same amount of ammonia[81]. However, plasma reactors eliminate the need for high-pressure systems, reducing initial investment costs by an order of magnitude (~US$0.54 million versus ~US$6.79 million for comparable small-scale units)[81]. If plasma synthesis achieves a large-scale conversion rate of 10%, hydrogen–ammonia energy storage systems based on both methods could offer comparable returns on investment, short payback periods and strong risk resilience[81]. The levelized cost of electricity for plasma synthesis is projected at US$0.062 per kilowatt-hour, which is lower than the Haber–Bosch process cost of US$0.069 per kilowatt-hour and below the US$0.064 per kilowatt-hour minimum electricity price[81]. Moreover, plasma's ambient operating conditions reduce material demands, enabling easier recycling and upgrades[81].

Compared with direct plasma catalysis, the tandem plasma-electrocatalysis process offers improved energy efficiency and cost-effectiveness[82]. The CAPEX are significantly lower than those for the Haber–Bosch process, as the tandem plasma-electrocatalysis process eliminates the need for high-pressure reactors and large-scale hydrogen production, making small-scale deployment more feasible[61]. However, the OPEX of this tandem approach are heavily influenced by electricity consumption, which accounts for approximately 90% of total production costs at an annual scale of ~10,000 tonne$_{NH3}$ (ref. 61). The LCOA for plasma-electrocatalysis is ~US$5,011 per tonne$_{NH3}$, with potential reductions to ~US$3,453 per tonne$_{NH3}$ through optimization[75]. At production capacities below 100 kg h^{-1}, this technology is already cost-competitive with the Haber–Bosch process based on green hydrogen at electricity prices of ~US$60 per megawatt-hour. Achieving parity at ~1 tonne$_{NH3}$ per hour would require an electricity price below ~US$20 per megawatt-hour[75].

Ammonia decomposition for hydrogen production

Ammonia, containing 17.5 wt% hydrogen, can be an effective hydrogen carrier, enabling storage and transportation of hydrogen energy[83–85]. Ammonia decomposition to produce hydrogen is an important intermediate step in ammonia-to-power conversion. Ammonia has a high auto-ignition temperature (651 °C) (Fig. 1d), making it difficult to efficiently sustain combustion in typical engines or burners under standard conditions (<350 °C)[86]. Hydrogen produced from partial ammonia decomposition can act as a combustion promoter, ensuring reliable and efficient combustion[87]. Complete ammonia decomposition can supply pure hydrogen for various energy conversion applications, such as hydrogen fuel cells and hydrogen-powered engines[88]. Ammonia cracking links synthesis and utilization, facilitating the on-demand generation of high-purity hydrogen at the point of use[89]. Although often regarded as a relatively mature technology, it continues to face persistent challenges, including the need for elevated operating temperatures and dependence on costly ruthenium-based catalysts[7,90–92].

Unlike the ammonia synthesis reaction, the decomposition of ammonia into hydrogen and nitrogen is an endothermic process ($2NH_3(g) \rightarrow 3H_2(g) + N_2(g)$, $\Delta H° = 92$ kJ mol^{-1}). Although the thermodynamic equilibrium predicts a near-complete ammonia conversion of 99% at 350 °C and atmospheric pressure, the actual energy consumption substantially surpasses theoretical values[93]. Ammonia decomposition typically requires external heating, operating at temperatures between 850 °C and 950 °C (refs. 94,95). Therefore, it demands pursuing efficient catalysts to run the reaction below 400 °C (ref. 90). The design principles for ammonia decomposition are markedly different from the synthesis reaction, even though both processes are reversible.

The dissociative adsorption of N_2 determines the catalytic activity of the metal in ammonia synthesis[96], which is related through the Brønsted–Evans–Polanyi relationship with the principle of microscopic reversibility (Supplementary Table 2). Although the principle of microscopic reversibility also applies to ammonia decomposition, the optimal binding energies of N_2 and NH_3 in ammonia synthesis and decomposition are substantially different[96] (Fig. 4a). The linear relationship between the adsorption energies of different nitrogen-containing species (NH_x, $x = 0, 1, 2$ and 3) on transition metal surfaces[96] suggests that nitrogen chemisorption energy can explain the reactivity of ammonia decomposition catalysts (Fig. 4b). Under typical reaction conditions (for example, 500 °C and 1 bar), ruthenium-based catalysts with an optimal nitrogen chemisorption energy exhibit excellent NH_3 decomposition performance (with the complete decomposition temperature range of 425–550 °C)[97]. The optimal nitrogen chemisorption strength ensures sufficiently strong adsorption to facilitate N–H bond cleavage, while avoiding excessive binding that would hinder N_2 desorption, thereby balancing the reaction kinetics across all elementary steps. However, ruthenium is a precious metal with low earth abundance, which limits large-scale application. Ammonia decomposition catalysts should achieve complete ammonia decomposition (typically >99%) at temperatures below 400 °C (refs. 97–104) (Fig. 4c and Supplementary Table 3).

Bimetallic alloy catalysts offer a potential strategy towards advanced catalysts with superior catalytic performance to their monometallic counterparts[100]. However, some bimetallic alloy catalysts, such as bimetallic Co–Mo catalyst, which shows a performance comparable with ruthenium-based catalysts, are limited in stability due to the large miscibility gap[96,105]. Cobalt-rich catalysts, such as high-entropy alloy catalyst (CoMoFeNiCu)[104], might help to balance metal miscibility and multifunctional performance due to their weak binding with *N (* represents a vacant active site on the catalyst surface) in relatively high kinetic barriers for dehydrogenation. Conversely, molybdenum-rich catalysts show excessively strong binding, hindering the recombination and desorption of *N from the surface of the catalyst[90].

Metal amide salts can catalyse ammonia decomposition through a chemical looping process[22]. The NH_3 decomposition reaction on these metal amide salts occurs via a Mars–van Krevelen mechanism, which is facilitated by the presence of anion (NH_2^-) vacancies on the imide substrate[106]. Among the various metal amide salt catalysts, the catalytic activity of $LiNH_2$–Ru–MgO in the ammonia decomposition reaction stands out[99] (Fig. 4c).

From the reaction perspective, high-pressure operation generally favours process intensification and pressurized H_2 for downstream utilization[107,108]. However, research on NH_3 decomposition at high pressures is scarce. Both catalyst and reactor design should be considered to optimize NH_3 decomposition at lower temperatures and higher pressures (<400 °C and >20 bar)[109].

Plasma reactors, photo-thermal reactors and electrolysers are currently at a TRL of less than 4 (ref. 110). Plasma reactors leverage high-energy plasma to provide additional energy to facilitate the activation and dissociation of ammonia molecules, lowering the energy barrier along the excited-state pathway[111,112]. Photo-thermal reactors integrate solar energy with thermal catalysis, harnessing sunlight photo-thermal effects to drive the decomposition reaction[113]. Ammonia electrolysers, coupled with ammonia oxidation and hydrogen production, can offer ultra-pure hydrogen without pressure swing adsorption separation[114].

Comparing the levelized cost of hydrogen (LOCH) of a fixed-bed reactor (Supplementary Fig. 1) and catalytic membrane reactors[110] shows that catalytic membrane reactors can eliminate the need for pressure swing adsorption separation and decrease the LOCH, based on an Aspen simulation (Fig. 4d, Supplementary Fig. 2 and Supplementary Tables 4 and 5). The LOCH is substantially influenced by the cost of ammonia feedstock, which is closely related to fluctuations in the raw material price of ammonia[115]. Our comparison of the LOCH sourced from green ammonia (US$450–500 per tonne$_{H2}$)[116], blue ammonia (US$150–180 per tonne$_{H2}$)[117] and grey ammonia (US$80–150 per tonne$_{H2}$) feedstocks[117] indicates that the hydrogen derived from green ammonia is priced at approximately double that of its grey and blue counterparts (Fig. 4d). However, as industrialization progresses and costs of renewable electricity and electrolysis technologies continue to decline[118], the price of green ammonia is anticipated to drop below the price of grey ammonia[119].

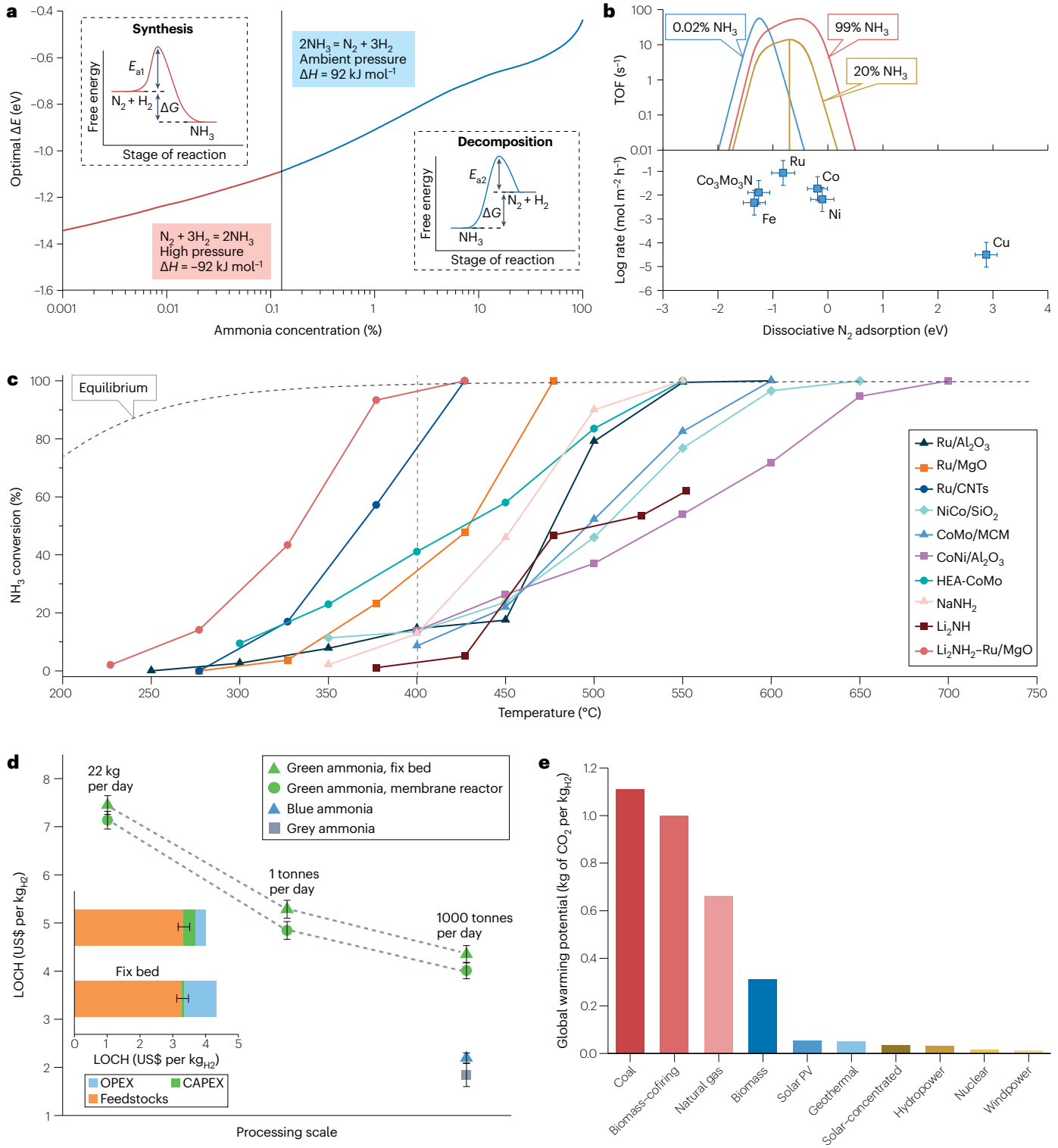

Traditional ammonia decomposition depends on the high thermal energy input. The conventional use of coal-fired routes in fixed-bed reactors results in carbon emissions that are two orders of magnitude higher compared with renewable energy sources, including solar, hydropower and wind energy[120] (Fig. 4e). With the development of renewable energy, wasted off-grid electricity and solar energy have been adopted to reduce the input of thermal energy[121].

Microreactors are characterized by their small channel dimensions (typically less than 500 μm) and feature intricate channel networks[122]. Within channels, gases are precisely manipulated to flow and react,

Fig. 4 | Catalyst design and economics of ammonia decomposition. a, The dissociative nitrogen (N_2) adsorption energy of an optimal catalyst for ammonia synthesis and decomposition at 500 °C, 1 bar and a 3:1 hydrogen (H_2):N_2 ratio corresponds to an equilibrium ammonia (NH_3) concentration of approximately 0.13%[96]. **b**, Turnover frequency (TOF) of ammonia synthesis and decomposition at 500 °C, 1 bar, a 3:1 H_2:N_2 ratio and different ammonia concentrations (0.02%, 20% and 99%) as a function of the dissociative nitrogen adsorption energy (top). Experimental reaction rates for ammonia decomposition at 500 °C, 1 bar and an equilibrium concentration of 20% NH_3 (bottom). The comparison of TOF profiles at varying ammonia concentrations shows that the optimal dissociative nitrogen adsorption energy shifts with ammonia partial pressure, indicating that the most active catalyst for ammonia synthesis or decomposition depends strongly on the reaction environment[96]. **c**, Comparison of different catalyst designs and catalytic performance in ammonia decomposition. Higher conversions at lower temperatures indicate superior catalytic performance, underscoring the decisive role of catalyst design in ammonia decomposition. The data used in the figure are from refs. 97–104 and are provided in Supplementary Table 3. **d**, The levelized cost of hydrogen (LOCH) assessment in two different reactors and an ammonia source with different scales. LOCH decreases markedly with increasing scale, with feedstock cost dominating at all scales and reactor choice having a minor impact relative to ammonia source. The expenditure for the operational and maintenance costs (OPEX) and capital expenditures (CAPEX) both pertain to a capacity of 1,000 tonnes per year. The data used in the figure are from ref. 110 and are provided in Supplementary Table 4. **e**, Global warming potential of different energy sources for hydrogen production through ammonia decomposition[120]. Fossil-based routes (coal, biomass-cofiring, natural gas) result in substantially higher carbon dioxide (CO_2) emissions per kilogram of hydrogen, whereas renewable and nuclear pathways can achieve near-zero emissions. Panels **a** and **b** adapted with permission from ref. 96, Elsevier. Panel **e** adapted with permission from ref. 120, Elsevier.

facilitating controlled chemical processes with excellent mass and heat transfer[123]. Joule heating reactors use the voltage applied to conductive materials to achieve rapid and efficient heating through the Joule effect. In addition, Joule heating reactors are relatively simple, as they do not require external furnaces or elaborate thermal management systems, making them suitable for industrial scale-up[124,125].

Ammonia fuel cells

An effective ammonia-to-power conversion requires optimizing the process of energy release from ammonia. This optimizing includes developing efficient technologies for combustion (power generation), fuel cells or other energy conversion systems that utilize ammonia[5]. The combustion efficiency of ammonia is lower compared with other fuels such as hydrogen, gasoline and diesel, which decreases its overall thermal efficiency[2]. In comparison with these combustion-based technologies, fuel cells can surpass the limitations of the Carnot cycle, achieving high theoretical efficiencies exceeding 80%[126]. Taking into consideration the feeding methods and operating temperature, ammonia fuel cells can be classified into three different operational modes: direct-ammonia fuel cells, indirect-ammonia fuel cells and ammonia SOFCs (Fig. 5a–c).

Direct-ammonia fuel cells use gaseous ammonia or its aqueous solution as the fuel source. Ammonia is oxidized to nitrogen on the anode side, requiring a theoretical cell voltage of 1.17 V, close to that of hydrogen fuel cells[127]. The ion exchange membrane is a crucial component of direct-ammonia fuel cells. In acidic environments, such as those in which a proton-exchange membrane is used, ammonia tends to transform into ammonium ions ($pK_a = 9.25$). This transformation makes it extremely difficult to oxidize ammonia due to the high energy barrier associated with the loss of its lone-pair electrons[128]. In contrast to a proton-exchange membrane, an AEM can offer hydroxide-enriched environments, overcoming the issues associated with the formation of ammonium ions[128]. Despite this advantage, AEM-type direct-ammonia fuel cells are also severely hindered by the sluggish kinetics characteristic of ammonia oxidation and ammonia crossover[129].

Regarding the catalytic mechanism in AEM-type direct-ammonia fuel cells, it is generally accepted that electrochemical ammonia oxidation follows the Oswin–Salomon or Gerische–Mauerer process[130] (Fig. 5d). The Oswin–Salomon mechanism describes ammonia dehydrogenating successively to form *N, and then two *N dimerize into N_2. The Gerische–Mauerer mechanism diverges in the dimerization step, using $*NH_x$ instead of *N. In the Gerische–Mauerer mechanism, $*NH_x$ dimerization is rate-determining[128]. Both theoretical calculations and experiments suggest that the Gerische–Mauerer mechanism is more feasible because strongly absorbed *N poisons at active sites make the coupling of N–N and desorption of N_2 less likely to happen in the Oswin–Salomon process[131,132]. However, active platinum catalysts that follow the Gerische–Mauerer pathway show an overpotential exceeding 400 mV, lagging behind hydrogen oxidation kinetics (<10 mV)[128]. Moreover, platinum catalysts are readily deactivated above 0.6 V due to *N deposition, leading to a narrow potential window for ammonia oxidation fuel cells[133].

In contrast to direct-ammonia fuel cells, hydrogen fuel cells are a developed and mature technology (TRL 9) for power generation[134]. As a hydrogen carrier, NH_3 can be catalytically converted into a gaseous admixture constituting 75% H_2 and 25% N_2, within an NH_3 thermal decomposition cracker (indirect-ammonia fuel cells)[135]. The anodic and cathodic reactions in indirect-ammonia fuel cells are identical to those in hydrogen fuel cells. The main drawback is the residual ammonia formed during the early-stage decomposition process. In proton-exchange membrane-type fuel cells, 10 ppm of residual ammonia can decrease the current to one-third of its original value[136]. The International Organization for Standardization has proposed an ammonia concentration limit as low as 0.1 ppm (ref. 137). Alternatively, AEM-type fuel cells can be used, as they are not highly sensitive to trace amounts of ammonia.

In contrast to low-temperature fuel cells, SOFCs usually operate in the temperature range between 500 °C and 800 °C, which overlaps with the decomposition temperature of ammonia[138]. For this reason, SOFCs do not need an additional cracker. In direct-ammonia SOFCs, the kinetic barriers of ammonia utilization are predominantly associated with the ammonia cracking process[138]. The ratio of the maximum power density achieved by SOFCs when fed with NH_3 and H_2 ($P_{max}NH_3$:$P_{max}H_2$) increases with temperature. The ratio of power density reflects the relative SOFCs performance on ammonia versus hydrogen, indicating the efficiency of in situ ammonia decomposition and electrochemical utilization. A higher ratio indicates that ammonia would decompose at a more rapid rate at elevated temperatures[139–143] (Fig. 5e). Despite the sluggish ammonia decomposition process, the direct-ammonia SOFCs can still achieve a P_{max} (maximum power density) value exceeding 1 W cm^{-2} under the direct-ammonia feeding mode, which is competitive with the most advanced proton-exchange membrane-type hydrogen fuel cells (1–1.5 W cm^{-2})[142]. However, the commonly used nickel-based catalysts (nickel–yttria-stabilized ZrO_2 (Ni-YSZ)) in direct-ammonia SOFCs

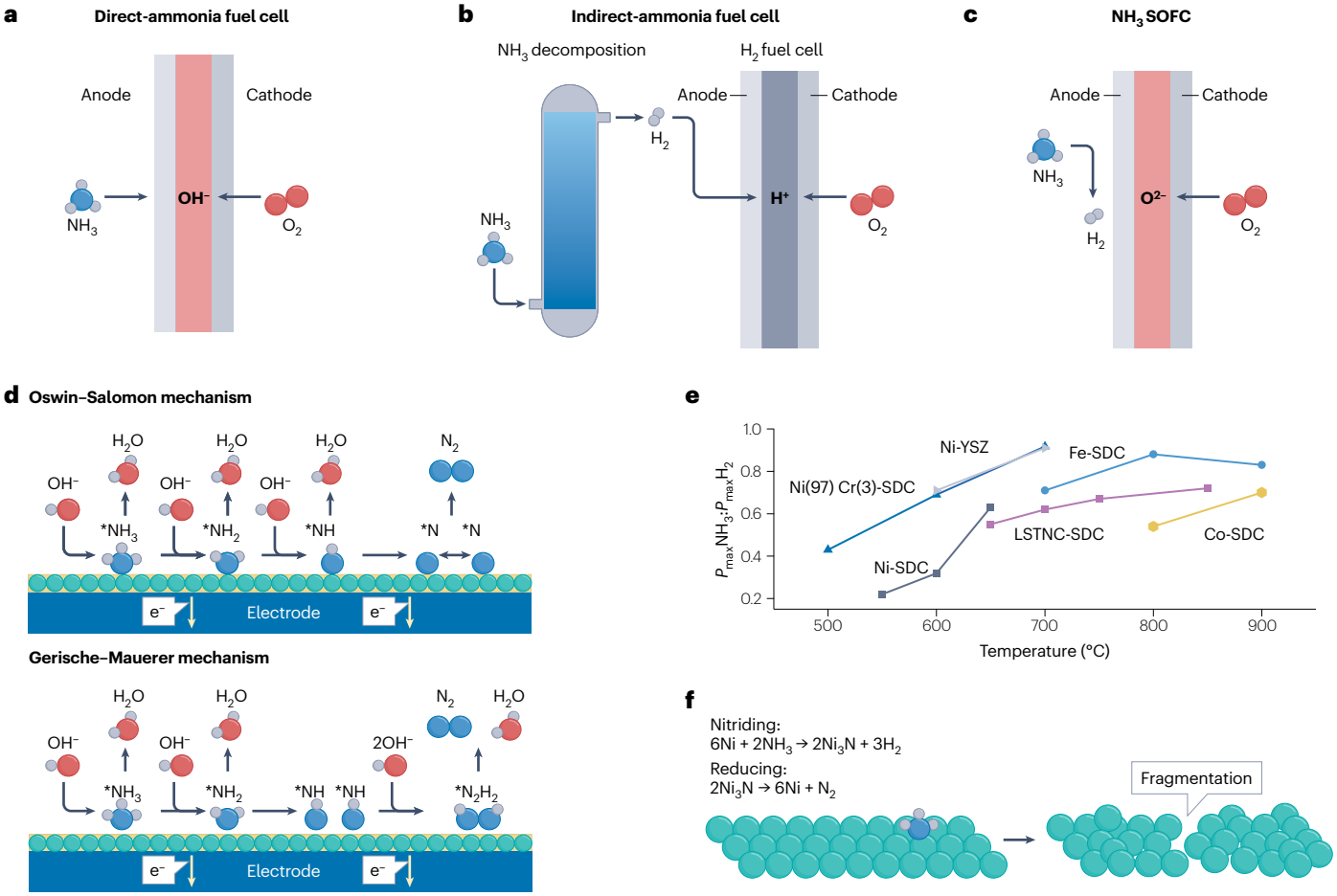

Fig. 5 | Mechanisms and operational strategies for ammonia fuel cells. **a**, In direct-ammonia (NH_3) fuel cells, ammonia oxidation occurs at the anode, producing nitrogen (N_2) and electrons, and hydroxide ions (OH^-) are transported through an anion exchange membrane (AEM). **b**, In indirect-ammonia fuel cells, ammonia is first cracked into hydrogen (H_2) and N_2 in an ammonia decomposition unit, and the resulting hydrogen is then used in a hydrogen fuel cell. This approach leverages the maturity of hydrogen fuel cells while addressing the challenges of direct ammonia oxidation by replacing the sluggish ammonia oxidation with the fast hydrogen oxidation reaction (HOR). **c**, High-temperature solid-oxide fuel cells (SOFCs) can directly use ammonia as a fuel, with ammonia thermally decomposing into H_2 and N_2 before the electrochemical oxidation at the anode. **d**, Ammonia oxidation mechanisms in AEM-type and direct-ammonia fuel cells, such as the Oswin–Salomon and Gerischer–Mauerer pathways, provide different routes for ammonia dehydrogenation and nitrogen release. **e**, The efficiency of ammonia-fed SOFCs at elevated temperatures increases due to enhanced NH_3 decomposition kinetics. The data used in the figure are from refs. 139–143. **f**, Nickel catalyst degradation mechanism in ammonia-fed SOFCs. Cyclic nitridation and reduction effects lead to catalyst deactivation, a key challenge limiting the long-term performance of SOFCs with direct ammonia feeding. * represents a vacant active site on the catalyst surface. LSTNC, NiCo alloy supported on $La_{0.55}Sr_{0.3}TiO_{3-\delta}$; $P_{max}NH_3$:$P_{max}H_2$, ratio of the maximum power density achieved by SOFCs when fed with NH_3 and H_2; SDC, Sm_2O_3-doped CeO_2; YSZ, yttria-stabilized ZrO_2.

undergo cyclic nitriding and reduction processes (Fig. 5f). As a result, direct-ammonia SOFCs are likely to experience more rapid catalyst degradation[144]. This degradation can be avoided in indirect-ammonia fuel cells as these do not generally experience kinetic and degradation issues[145].

Taking into account different parameters such as technological maturity, energy efficiency and CO_2 emissions, an ammonia-based economy requires relatively mature and cost-effective technological solutions, such as green hydrogen production and Haber–Bosch ammonia synthesis[134]. From a power-to-ammonia-to-power perspective, the round-trip efficiency (RTE) of each ammonia utilization pathway is evaluated by comparing the cumulative energy input required across all technological steps with the net usable electrical output delivered at the endpoint[146]. When ammonia is directly fed into a SOFC, the RTE reaches 21% (Fig. 6a). Notably, incorporating an ammonia cracking step prior to the fuel cell substantially improves energy efficiency. In pathways in which ammonia is first thermally decomposed into hydrogen and then utilized in a fuel cell, either at ambient or elevated temperatures, the RTE increases to 26% for the indirect-ammonia fuel cell system (cracker and low-temperature fuel cell) and further to 28% for the cracker and SOFC configuration. Moreover, fuel cell-based routes exhibit substantially higher round-trip efficiencies compared with combustion-based technologies, such as internal combustion engines (ICEs) and gas turbines[146] (Fig. 6b).

At an electricity price of approximately US$0.15 per kilowatt-hour in the United States, renewable power sources must be priced below US$0.04 per kilowatt-hour (RTE 28%) to ensure that ammonia-based energy systems remain cost-competitive and economically attractive[147]. Building on this near-future scenario (Supplementary Table 6), we further compared the cost per megajoule of energy delivered by fuel cells with that of NH_3-fuelled ICEs, NH_3 turbines and lithium-ion batteries. The fuel cell pathway, in particular the cracked NH_3-SOFC system, achieves a remarkably low energy cost of US$0.03 per megajoule, comparable with that of lithium-ion batteries charged from the electrical grid[148] (Supplementary Table 7).

Summary and future perspectives

Ammonia has emerged as a versatile energy carrier with potential for large-scale renewable energy storage and utilization. Despite advancements in decentralized ammonia synthesis under mild conditions, decomposition for hydrogen production and direct utilization in energy conversion technologies such as fuel cells, several critical challenges must be addressed to enable ammonia's widespread adoption in energy systems. Within the next 5 years, efforts should prioritize the development of selective and durable catalysts, achieving selectivity above 90% in continuous-flow systems, along with the establishment of standardized benchmarking protocols specifying the anodic coupling reaction, applied current density, electrolyte composition, cell voltage, electrode area and cell configuration under defined operating conditions. In 10 years, the field is expected to deliver integrated reactor–separator platforms that combine renewable hydrogen, scalable synthesis and energy-efficient ammonia recovery, with production rates exceeding 1,000 nmol cm^{-2} s^{-1} and energy consumption below 30 GJ per $tonne_{NH3}$ (refs. 4,17). Over the next 20 years and beyond, successful deployment at distributed or industrial scales will depend on holistic system optimization — spanning catalyst design, separation efficiency, storage and regulatory integration — to position green ammonia as a viable alternative to the conventional Haber–Bosch process[4].

Decentralized ammonia synthesis methods, including electrochemical and plasma-assisted processes, remain at early TRLs (TRL1–4), requiring substantial improvements in efficiency, scalability and stability to become industrially viable. Achieving high FE, energy efficiency exceeding 30% and long-term operational stability is essential for electrochemical ammonia production to reach cost-competitiveness with the Haber–Bosch process. Additionally, optimizing plasma-catalytic systems to enhance ammonia yields while reducing energy consumption is needed for advancing non-thermal pathways. From an economic perspective, lithium-mediated ammonia synthesis shows potential, particularly for small-scale applications, in which production costs can be as low as US$700 per $tonne_{NH3}$. With continued advancements in electrochemical synthesis, decentralized ammonia production could reduce the dependence on centralized Haber–Bosch plants and extensive supply chains, making ammonia production more adaptable to the intermittent and distributed nature of renewable energy. To achieve cost-competitiveness, further improvements in catalyst design, reactor engineering and process integration are essential for

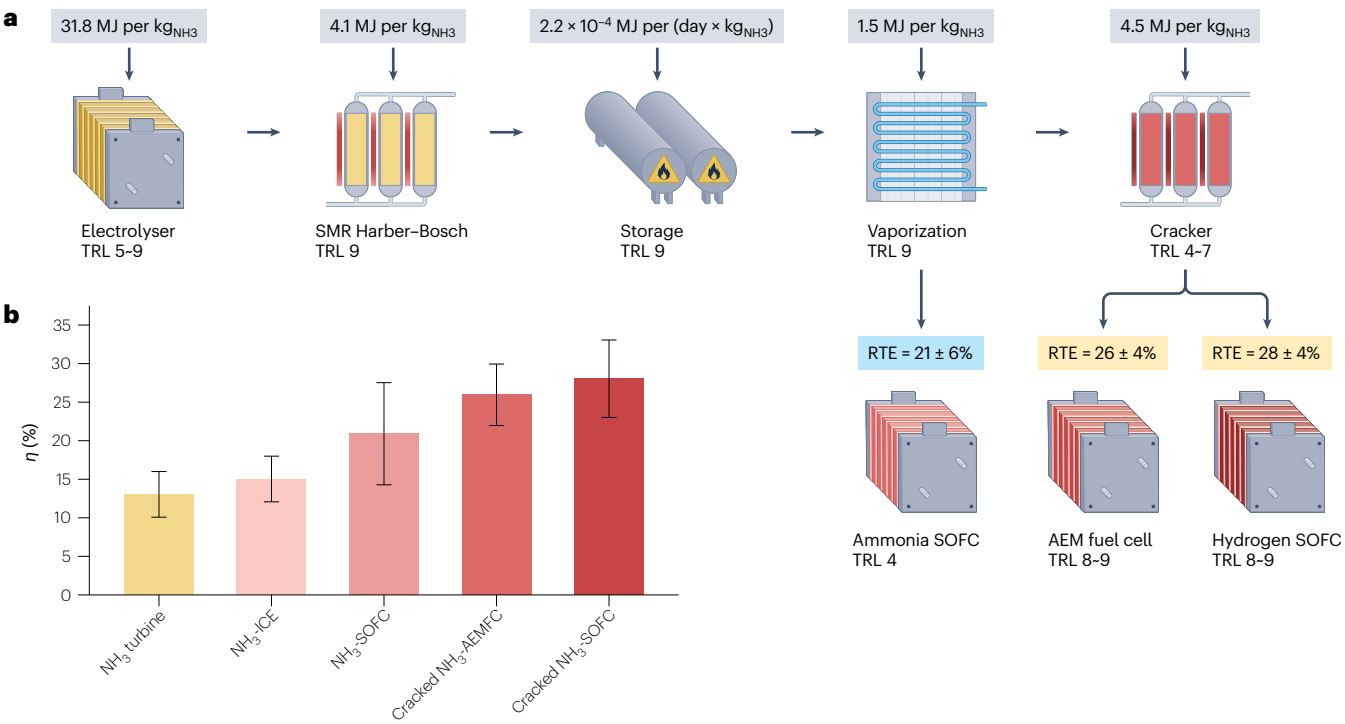

Fig. 6 | Efficiency of ammonia fuel cell technologies. a, Round-trip efficiency (RTE) of power-to-ammonia-to-power systems, including direct-ammonia solid-oxide fuel cells (SOFCs), indirect-ammonia fuel cells and hydrogen fuel cells. Efficiency values underscore the trade-offs between ammonia cracking and direct oxidation approaches. The RTE reflects the overall energy efficiency of the process, with higher values indicating superior technological performance. **b**, RTE of ammonia-fed fuel cells and alternative ammonia utilization methods, such as internal combustion engines (ICEs) and gas turbines, with electrochemical conversion processes demonstrating superior efficiency[146]. AEM, anion exchange membrane; SMR, steam methane reforming; TRL, technology readiness level. Panel **b** adapted with permission from ref. 146, Elsevier.

lowering both capital and operational costs, ultimately positioning green ammonia as a viable alternative.

For ammonia-to-hydrogen conversion, the efficiency and cost-effectiveness of catalytic ammonia decomposition must be further improved. Developing robust, low-cost catalysts that enable complete ammonia conversion at temperatures below 400 °C is a key priority. High-entropy alloy catalysts and chemical looping strategies offer pathways for achieving lower-temperature operation while maintaining high conversion rates. Additionally, reactor designs that integrate heat recovery and advanced separation technologies could improve the economic feasibility of ammonia decomposition for hydrogen production. In energy conversion technologies, ammonia fuel cells, including direct-ammonia fuel cells and SOFCs, present notable opportunities but require advances in catalyst stability, ammonia oxidation kinetics and membrane durability to enhance efficiency and reliability. Addressing ammonia crossover and NO_x formation in fuel cells is critical to achieving high-performance, low-emission power generation. Meanwhile, ammonia combustion technologies need optimized burners, and turbine designs to mitigate NO_x emissions and improve combustion stability.

Investment in pilot-scale demonstrations, improved regulatory frameworks and cross-sector collaborations will be essential to accelerating commercialization. Addressing ammonia's challenges holistically by advancing synthesis efficiency, optimizing utilization technologies and ensuring economic feasibility will position ammonia as a key enabler in the transition to a low-carbon energy future.

Published online: 10 September 2025

References

1. Al-Shetwi, A. Q., Abidin, I. Z., Mahafzah, K. A. & Hannan, M. A. Feasibility of future transition to 100% renewable energy: recent progress, policies, challenges, and perspectives. *J. Clean. Prod.* **478**, 143942 (2024).
2. Valera-Medina, A., Xiao, H., Owen-Jones, M., David, W. I. F. & Bowen, P. J. Ammonia for power. *Prog. Energy Combust. Sci.* **69**, 63–102 (2018).
3. Gür, T. M. Review of electrical energy storage technologies, materials and systems: challenges and prospects for large-scale grid storage. *Energy Environ. Sci.* **11**, 2696–2767 (2018).
4. MacFarlane, D. R. et al. A roadmap to the ammonia economy. *Joule* **4**, 1186–1205 (2020).
5. Yapicioglu, A. & Dincer, I. A review on clean ammonia as a potential fuel for power generators. *Renew. Sustain. Energy Rev.* **103**, 96–108 (2019).
6. Guo, J. P. & Chen, P. Catalyst: NH_3 as an energy carrier. *Chem* **3**, 709–712 (2017).
7. Spatolisano, E., Pellegrini, L. A., de Angelis, A. R., Cattaneo, S. & Roccaro, E. Ammonia as a carbon-free energy carrier: NH_3 cracking to H_2. *Ind. Eng. Chem. Res.* **62**, 10813–10827 (2023).
8. David, W. I. F. et al. 2023 roadmap on ammonia as a carbon-free fuel. *JPhys Energy* **6**, 021501 (2024).
9. The Royal Society. *Ammonia: Zero-Carbon Fertiliser, Fuel and Energy Store* (The Royal Society, 2020).
10. Kobayashi, H., Hayakawa, A., Somarathne, K. D. K. A. & Okafor, E. C. Science and technology of ammonia combustion. *Proc. Combust. Inst.* **37**, 109–133 (2019).
11. Westhead, O. et al. Near ambient N_2 fixation on solid electrodes versus enzymes and homogeneous catalysts. *Nat. Rev. Chem.* **7**, 184–201 (2023).
12. Iriawan, H. et al. Methods for nitrogen activation by reduction and oxidation. *Nat. Rev. Methods Primers* **1**, 56 (2021).
13. Chang, W. S., Jain, A., Rezaie, F. & Manthiram, K. Lithium-mediated nitrogen reduction to ammonia via the catalytic solid-electrolyte interphase. *Nat. Catal.* **7**, 231–241 (2024).
14. Li, S., Fu, X., Nørskov, J. K. & Chorkendorff, I. Towards sustainable metal-mediated ammonia electrosynthesis. *Nat. Energy* **9**, 1344–1349 (2024).
15. Wang, Y. et al. Shielding protection by mesoporous catalysts for improving plasma-catalytic ambient ammonia synthesis. *J. Am. Chem. Soc.* **144**, 12020–12031 (2022).
16. Fu, X. B., Zhang, J. H. & Kang, Y. J. Recent advances and challenges of electrochemical ammonia synthesis. *Chem. Catal.* **2**, 2590–2613 (2022).
17. Fu, X. & Chorkendorff, I. Prospects and challenges in electrochemical nitrogen activation for ammonia synthesis. *Sci. China Chem.* **67**, 3510–3514 (2024).
18. Erisman, J. W., Sutton, M. A., Galloway, J., Klimont, Z. & Winiwarter, W. How a century of ammonia synthesis changed the world. *Nat. Geosci.* **1**, 636–639 (2008).
19. Li, K. et al. Enhancement of lithium-mediated ammonia synthesis by addition of oxygen. *Science* **374**, 1593–1597 (2021).
20. Fernández, C. A., Chapman, O., Brown, M. A., Alvarez-Pugliese, C. E. & Hatzell, M. C. Achieving decentralized, electrified, and decarbonized ammonia production. *Environ. Sci. Technol.* **58**, 6964–6977 (2024).
21. Ithisuphalap, K. et al. Photocatalysis and photoelectrocatalysis methods of nitrogen reduction for sustainable ammonia synthesis. *Small Methods* **3**, 1800352 (2019).
22. Gao, W. B. et al. Production of ammonia via a chemical looping process based on metal imides as nitrogen carriers. *Nat. Energy* **3**, 1067–1075 (2018).
23. Tanifuji, K. & Ohki, Y. Metal-sulfur compounds in N_2 reduction and nitrogenase-related chemistry. *Chem. Rev.* **120**, 5194–5251 (2020).
24. Andersen, S. Z. et al. A rigorous electrochemical ammonia synthesis protocol with quantitative isotope measurements. *Nature* **570**, 504–508 (2019).
25. Mehta, P. et al. Overcoming ammonia synthesis scaling relations with plasma-enabled catalysis. *Nat. Catal.* **1**, 269–275 (2018).
26. Han, G.-F. et al. Mechanochemistry for ammonia synthesis under mild conditions. *Nat. Nanotechnol.* **16**, 325–330 (2021).
27. Choi, J. et al. Identification and elimination of false positives in electrochemical nitrogen reduction studies. *Nat. Commun.* **11**, 5546 (2020).
28. Lazouski, N., Schiffer, Z. J., Williams, K. & Manthiram, K. Understanding continuous lithium-mediated electrochemical nitrogen reduction. *Joule* **3**, 1127–1139 (2019).
29. Fu, X. et al. Continuous-flow electrosynthesis of ammonia by nitrogen reduction and hydrogen oxidation. *Science* **379**, 707–712 (2023).
30. Westhead, O. et al. The role of ion solvation in lithium mediated nitrogen reduction. *J. Mater. Chem. A* **11**, 12746–12758 (2023).
31. Fu, X. B. et al. Calcium-mediated nitrogen reduction for electrochemical ammonia synthesis. *Nat. Mater.* **23**, 101–107 (2024).
32. Lazouski, N., Chung, M. J., Williams, K., Gala, M. L. & Manthiram, K. Non-aqueous gas diffusion electrodes for rapid ammonia synthesis from nitrogen and water-splitting-derived hydrogen. *Nat. Catal.* **3**, 463–469 (2020).
33. Schwalbe, J. A. et al. A combined theory–experiment analysis of the surface species in lithium-mediated NH_3 electrosynthesis. *ChemElectroChem* **7**, 1542–1549 (2020).
34. Cai, X. Y. et al. Membrane electrode assembly design for lithium-mediated electrochemical nitrogen reduction. *Energy Environ. Sci.* **16**, 3063–3073 (2023).
35. Li, S. et al. Electrosynthesis of ammonia with high selectivity and high rates via engineering of the solid-electrolyte interphase. *Joule* **6**, 2083–2101 (2022).
36. Du, H. L. et al. Electroreduction of nitrogen with almost 100% current-to-ammonia efficiency. *Nature* **609**, 722–727 (2022).
37. Fu, X. Lithium-mediated nitrogen reduction for electrochemical ammonia synthesis: from batch to flow reactor. *Mater. Today Catal.* **3**, 100031 (2023).
38. Fu, X. B. et al. Phenol as proton shuttle and buffer for lithium-mediated ammonia electrosynthesis. *Nat. Commun.* **15**, 2417 (2024).
39. Cai, X. Y. et al. Lithium-mediated electrochemical nitrogen reduction: mechanistic insights to enhance performance. *iScience* **24**, 103105 (2021).
40. Li, K. et al. Increasing current density of Li-mediated ammonia synthesis with high surface area copper electrodes. *ACS Energy Lett.* **7**, 36–41 (2022).
41. Gao, L. F. et al. Domino effect: gold electrocatalyzing lithium reduction to accelerate nitrogen fixation. *Angew. Chem. Int. Ed.* **60**, 5257–5261 (2021).
42. Li, S. F. et al. Long-term continuous ammonia electrosynthesis. *Nature* **629**, 92–97 (2024).
43. Suryanto, B. H. R. et al. Nitrogen reduction to ammonia at high efficiency and rates based on a phosphonium proton shuttle. *Science* **372**, 1187–1191 (2021).
44. Tsuneto, A., Kudo, A. & Sakata, T. Efficient electrochemical reduction of N_2 to NH_3 catalyzed by lithium. *Chem. Lett.* **22**, 851–854 (1993).
45. Hyung et al. Utilizing water as a proton source for sustainable Li-mediated electrochemical ammonia synthesis. *Chem. Eng. J.* **497**, 154644 (2024).
46. Farghali, M. et al. Strategies for ammonia recovery from wastewater: a review. *Environ. Chem. Lett.* **22**, 2699–2751 (2024).
47. Lee, G., Kim, K., Chung, J. & Han, J.-I. Electrochemical ammonia accumulation and recovery from ammonia-rich livestock wastewater. *Chemosphere* **270**, 128631 (2021).
48. Lee, G., Kim, D. & Han, J.-I. Gas-diffusion-electrode based direct electro-stripping system for gaseous ammonia recovery from livestock wastewater. *Water Res.* **196**, 117012 (2021).
49. Iddya, A. et al. Efficient ammonia recovery from wastewater using electrically conducting gas stripping membranes. *Environ. Sci. Nano* **7**, 1759–1771 (2020).
50. Fu, X. What insights can we learn from dimensionally stable anodes (DSAs)? *Carbon Future* **1**, 9200027 (2024).
51. Wang, Y. et al. Engineering Ni–Co bimetallic interfaces for ambient plasma-catalytic CO_2 hydrogenation to methanol. *Chem* **10**, 2590–2606 (2024).
52. Chen, J. G. et al. Beyond fossil fuel-driven nitrogen transformations. *Science* **360**, eaar6611 (2018).
53. Kim, H.-H., Teramoto, Y., Ogata, A., Takagi, H. & Nanba, T. Atmospheric-pressure nonthermal plasma synthesis of ammonia over ruthenium catalysts. *Plasma Process. Polym.* **14**, 1600157 (2017).
54. Akay, G. & Zhang, K. Process intensification in ammonia synthesis using novel coassembled supported microporous catalysts promoted by nonthermal plasma. *Ind. Eng. Chem. Res.* **56**, 457–468 (2017).
55. Rouwenhorst, K. H. R., Mani, S. & Lefferts, L. Improving the energy yield of plasma-based ammonia synthesis with in situ adsorption. *ACS Sustain. Chem. Eng.* **10**, 1994–2000 (2022).
56. Peng, P. et al. Atmospheric plasma-assisted ammonia synthesis enhanced via synergistic catalytic absorption. *ACS Sustain. Chem. Eng.* **7**, 100–104 (2018).
57. Winter, L. R. & Chen, J. G. N_2 fixation by plasma-activated processes. *Joule* **5**, 300–315 (2021).

58. Abdelaziz, A. A., Teramoto, Y., Nozaki, T. & Kim, H.-H. Performance of high-frequency spark discharge for efficient NO production with tunable selectivity. *Chem. Eng. J.* **470**, 144182 (2023).
59. Liu, H. et al. Low-coordination rhodium catalysts for an efficient electrochemical nitrate reduction to ammonia. *ACS Catal.* **13**, 1513–1521 (2023).
60. Liu, W. et al. Efficient ammonia synthesis from the air using tandem non-thermal plasma and electrocatalysis at ambient conditions. *Nat. Commun.* **15**, 3524 (2024).
61. Guo, X. et al. Highly stable perovskite oxides for electrocatalytic acidic NO_x^- reduction streamlining ammonia synthesis from air. *Angew. Chem. Int. Ed.* **63**, e202410517 (2024).
62. Liu, H., Bai, L., Bergmann, A., Cuenya, B. R. & Luo, J. Electrocatalytic reduction of nitrogen oxide species to ammonia. *Chem* **10**, 2963–2986 (2024).
63. Hermawan, A., Alviani, V. N., Wibisono & Seh, Z. W. Fundamentals, rational catalyst design, and remaining challenges in electrochemical NO_x reduction reaction. *iScience* **26**, 107410 (2023).
64. Smith, C., Hill, A. K. & Torrente-Murciano, L. Current and future role of Haber–Bosch ammonia in a carbon-free energy landscape. *Energy Environ. Sci.* **13**, 331–344 (2020).
65. Rafiqul, I., Weber, C., Lehmann, B. & Voss, A. Energy efficiency improvements in ammonia production—perspectives and uncertainties. *Energy* **30**, 2487–2504 (2005).
66. Erfani, N., Baharudin, L. & Watson, M. Recent advances and intensifications in Haber–Bosch ammonia synthesis process. *Chem. Eng. Process.* **204**, 109962 (2024).
67. Jin, D. L., Chen, A. Q. & Lin, B. L. What metals should be used to mediate electrosynthesis of ammonia from nitrogen and hydrogen from a thermodynamic standpoint? *J. Am. Chem. Soc.* **146**, 12320–12323 (2024).
68. Kim, K. et al. Electrochemical synthesis of ammonia from water and nitrogen: a lithium-mediated approach using lithium-ion conducting glass ceramics. *ChemSusChem* **11**, 120–124 (2018).
69. Murphy, E. et al. Elucidating electrochemical nitrate and nitrite reduction over atomically-dispersed transition metal sites. *Nat. Commun.* **14**, 4554 (2023).
70. Ge, X. et al. Controlling the reaction pathways of mixed NO_xH_y reactants in plasma-electrochemical ammonia synthesis. *J. Am. Chem. Soc.* **146**, 35305–35312 (2024).
71. Buchner, G. A., Zimmermann, A. W., Hohgräve, A. E. & Schomäcker, R. Techno-economic assessment framework for the chemical industry—based on technology readiness levels. *Ind. Eng. Chem. Res.* **57**, 8502–8517 (2018).
72. Rezaie, F., Læsaa, S., Sahin, N. E., Catalano, J. & Dražević, E. Low-temperature electrochemical ammonia synthesis: measurement reliability and comparison to Haber–Bosch in terms of energy efficiency. *Energy Technol.* **11**, 2300410 (2023).
73. Li, X. et al. Synergistic catalysis of the synthesis of ammonia with Co-based catalysts and plasma: from nanoparticles to a single atom. *ACS Appl. Mater. Interfaces* **13**, 52498–52507 (2021).
74. Li, L. et al. Efficient nitrogen fixation to ammonia through integration of plasma oxidation with electrocatalytic reduction. *Angew. Chem. Int. Ed.* **60**, 14131–14137 (2021).
75. Wu, A. et al. Direct ammonia synthesis from the air via gliding arc plasma integrated with single atom electrocatalysis. *Appl. Catal. B* **299**, 120667 (2021).
76. Sun, J. et al. A hybrid plasma electrocatalytic process for sustainable ammonia production. *Energy Environ. Sci.* **14**, 865–872 (2021).
77. Zheng, J. et al. Enhanced NH_3 synthesis from air in a plasma tandem-electrocatalysis system using plasma-engraved N-doped defective MoS_2. *JACS Au* **3**, 1328–1336 (2023).
78. Fernandez, C. A. & Hatzell, M. C. Economic considerations for low-temperature electrochemical ammonia production: achieving Haber–Bosch parity. *J. Electrochem. Soc.* **167**, 143504 (2020).
79. Gomez, J. R. & Garzon, F. Preliminary economics for green ammonia synthesis via lithium mediated pathway. *Int. J. Energy Res.* **45**, 13461–13470 (2021).
80. Lazouski, N. et al. Cost and performance targets for fully electrochemical ammonia production under flexible operation. *ACS Energy Lett.* **7**, 2627–2633 (2022).
81. Chen, X. et al. Technical and economic analysis of renewable energy systems with hydrogen–ammonia energy storage: a comparison of different ammonia synthesis methods. *J. Energy Storage* **113**, 115549 (2025).
82. Wang, W., Wang, Y. & Tu, X. Tandem plasma electrocatalysis: an emerging pathway for sustainable ammonia production. *Curr. Opin. Green Sustain. Chem.* **51**, 100986 (2025).
83. Ganley, J. C., Thomas, F. S., Seebauer, E. G. & Masel, R. I. A priori catalytic activity correlations: the difficult case of hydrogen production from ammonia. *Catal. Lett.* **96**, 117–122 (2004).
84. Choudhary, T. V., Sivadinarayana, C. & Goodman, D. W. Catalytic ammonia decomposition: CO_x-free hydrogen production for fuel cell applications. *Catal. Lett.* **72**, 197–201 (2001).
85. Yin, S. F. et al. Investigation on the catalysis of CO-free hydrogen generation from ammonia. *J. Catal.* **224**, 384–396 (2004).
86. Wijayanta, A. T., Oda, T., Purnomo, C. W., Kashiwagi, T. & Aziz, M. Liquid hydrogen, methylcyclohexane, and ammonia as potential hydrogen storage: comparison review. *Int. J. Hydrog. Energy* **44**, 15026–15044 (2019).
87. Lucentini, I., Garcia, X., Vendrell, X. & Llorca, J. Review of the decomposition of ammonia to generate hydrogen. *Ind. Eng. Chem. Res.* **60**, 18560–18611 (2021).
88. Lee, J. E., Lee, J., Jeong, H., Park, Y.-K. & Kim, B.-S. Catalytic ammonia decomposition to produce hydrogen: a mini-review. *Chem. Eng. J.* **475**, 146108 (2023).
89. Babar, P. & Botte, G. G. Recent advances in ammonia electrolysis for sustainable hydrogen generation. *ACS Sustain. Chem. Eng.* **12**, 13030–13047 (2024).
90. Zecher-Freeman, N., Zong, H., Xie, P. & Wang, C. Catalytic cracking of ammonia toward carbon-neutral liquid fuel. *Curr. Opin. Green Sustain. Chem.* **44**, 100860 (2023).
91. Trangwachirachai, K., Rouwenhorst, K., Lefferts, L. & Faria Albanese, J. A. Recent progress on ammonia cracking technologies for scalable hydrogen production. *Curr. Opin. Green Sustain. Chem.* **49**, 100945 (2024).
92. Andriani, D. & Bicer, Y. A review of hydrogen production from onboard ammonia decomposition: maritime applications of concentrated solar energy and boil-off gas recovery. *Fuel* **352**, 128900 (2023).
93. Cao, C.-F. et al. Electronic metal–support interaction enhanced ammonia decomposition efficiency of perovskite oxide supported ruthenium. *Chem. Eng. Sci.* **257**, 117719 (2022).
94. Mukherjee, S., Devaguptapu, S. V., Sviripa, A., Lund, C. R. F. & Wu, G. Low-temperature ammonia decomposition catalysts for hydrogen generation. *Appl. Catal., B* **226**, 162–181 (2018).
95. Schüth, F., Palkovits, R., Schlögl, R. & Su, D. S. Ammonia as a possible element in an energy infrastructure: catalysts for ammonia decomposition. *Energy Environ. Sci.* **5**, 6278–6289 (2012).
96. Boisen, A., Dahl, S., Norskov, J. & Christensen, C. Why the optimal ammonia synthesis catalyst is not the optimal ammonia decomposition catalyst. *J. Catal.* **230**, 309–312 (2005).
97. Yin, S. F., Xu, B. Q., Wang, S. J., Ng, C. F. & Au, C. T. Magnesia–carbon nanotubes (MgO–CNTs) nanocomposite: novel support of Ru catalyst for the generation of CO_x-free hydrogen from ammonia. *Catal. Lett.* **96**, 113–116 (2004).
98. David, W. I. F. et al. Hydrogen production from ammonia using sodium amide. *J. Am. Chem. Soc.* **136**, 13082–13085 (2014).
99. Guo, J. et al. Electronic promoter or reacting species? The role of $LiNH_2$ on Ru in catalyzing NH_3 decomposition. *Chem. Commun.* **51**, 15161–15164 (2015).
100. Wu, Z.-W. et al. Ammonia decomposition over SiO_2-supported Ni–Co bimetallic catalyst for CO_x-free hydrogen generation. *Int. J. Hydrog. Energy* **45**, 15263–15269 (2020).
101. Duan, X., Qian, G., Zhou, X., Chen, D. & Yuan, W. MCM-41 supported CoMo bimetallic catalysts for enhanced hydrogen production by ammonia decomposition. *Chem. Eng. J.* **207–208**, 103–108 (2012).
102. Fu, E. et al. Enhanced NH_3 decomposition for H_2 production over bimetallic M(M=Co, Fe, Cu)Ni/Al_2O_3. *Fuel Process. Technol.* **221**, 106945 (2021).
103. Guo, J. et al. Lithium imide synergy with 3d transition-metal nitrides leading to unprecedented catalytic activities for ammonia decomposition. *Angew. Chem. Int. Ed.* **54**, 2950–2954 (2015).
104. Xie, P. et al. Highly efficient decomposition of ammonia using high-entropy alloy catalysts. *Nat. Commun.* **10**, 4011 (2019).
105. Boisen, A., Dahl, S. & Jacobsen, C. J. H. Promotion of binary nitride catalysts: isothermal N_2 adsorption, microkinetic model, and catalytic ammonia synthesis activity. *J. Catal.* **208**, 180–186 (2002).
106. Ogasawara, K. et al. Ammonia decomposition over CaNH-supported Ni catalysts via an NH^{2-}-vacancy-mediated Mars–van Krevelen mechanism. *ACS Catal.* **11**, 11005–11015 (2021).
107. Strasser, P. et al. Lattice-strain control of the activity in dealloyed core–shell fuel cell catalysts. *Nat. Chem.* **2**, 454–460 (2010).
108. Sayas, S. et al. High pressure ammonia decomposition on Ru–K/CaO catalysts. *Catal. Sci. Technol.* **10**, 5027–5035 (2020).
109. Zhai, L., Liu, S. & Xiang, Z. Ammonia as a carbon-free hydrogen carrier for fuel cells: a perspective. *Ind. Chem. Mater.* **1**, 332–342 (2023).
110. Kanaan, R., Nóbrega, P. H. A., Achard, P. & Beauger, C. Economical assessment comparison for hydrogen reconversion from ammonia using thermal decomposition and electrolysis. *Renew. Sustain. Energy Rev.* **188**, 113784 (2023).
111. Mehta, P., Barboun, P., Go, D. B., Hicks, J. C. & Schneider, W. F. Catalysis enabled by plasma activation of strong chemical bonds: a review. *ACS Energy Lett.* **4**, 1115–1133 (2019).
112. Zeng, X. et al. Energy-efficient pathways for pulsed-plasma-activated sustainable ammonia synthesis. *ACS Sustain. Chem. Eng.* **11**, 1110–1120 (2023).
113. Li, J. et al. Utilizing full-spectrum sunlight for ammonia decomposition to hydrogen over GaN nanowires-supported Ru nanoparticles on silicon. *Nat. Commun.* **15**, 7393 (2024).
114. Zhang, K. et al. Energy-efficient and cost-effective ammonia electrolysis for converting ammonia to green hydrogen. *Cell Rep. Phys. Sci.* **5**, 102171 (2024).
115. Hatton, L., Bañares-Alcántara, R., Sparrow, S., Lott, F. & Salmon, N. Assessing the impact of climate change on the cost of production of green ammonia from offshore wind. *Int. J. Hydrog. Energy* **49**, 635–643 (2024).
116. Zhang, H., Wang, L., van Herle, J., Maréchal, F. & Desideri, U. Techno-economic comparison of green ammonia production processes. *Appl. Energy* **259**, 114135 (2020).
117. Oh, S., Mun, H., Park, J. & Lee, I. Techno-economic comparison of ammonia production processes under various carbon tax scenarios for the economic transition from grey to blue ammonia. *J. Clean. Prod.* **434**, 139909 (2024).
118. Lee, B. et al. Pathways to a green ammonia future. *ACS Energy Lett.* **7**, 3032–3038 (2022).
119. Cloete, S., Khan, M. N., Nazir, S. M. & Amini, S. Cost-effective clean ammonia production using membrane-assisted autothermal reforming. *Chem. Eng. J.* **404**, 126550 (2021).
120. Devkota, S. et al. Techno-economic and environmental assessment of hydrogen production through ammonia decomposition. *Appl. Energy* **358**, 122605 (2024).
121. Sen, R. & Bhattacharyya, S. C. Off-grid electricity generation with renewable energy technologies in India: an application of HOMER. *Renew. Energy* **62**, 388–398 (2014).
122. Sørensen, R. Z. et al. Promoted Ru on high-surface area graphite for efficient miniaturized production of hydrogen from ammonia. *Catal. Lett.* **112**, 77–81 (2006).
123. Gyak, K.-W. et al. 3D-printed monolithic SiCN ceramic microreactors from a photocurable preceramic resin for the high temperature ammonia cracking process. *React. Chem. Eng.* **4**, 1393–1399 (2019).

124. Badakhsh, A. et al. A compact catalytic foam reactor for decomposition of ammonia by the Joule-heating mechanism. *Chem. Eng. J.* **426**, 130802 (2021).
125. Liu, W. et al. Innovative internal Joule-heated reactor design: toward enhanced efficiency in hydrogen production via ammonia decomposition. *Chem. Eng. Sci.* **315**, 121906 (2025).
126. Lutz, A. E., Larson, R. S. & Keller, J. O. Thermodynamic comparison of fuel cells to the Carnot cycle. *Int. J. Hydrog. Energy* **27**, 1103–1111 (2002).
127. Chan, Y. T., Siddharth, K. & Shao, M. Investigation of cubic Pt alloys for ammonia oxidation reaction. *Nano Res.* **13**, 1920–1927 (2020).
128. Jiao, F. & Xu, B. Electrochemical ammonia synthesis and ammonia fuel cells. *Adv. Mater.* **31**, 1805173 (2019).
129. Bunce, N. J. & Bejan, D. Mechanism of electrochemical oxidation of ammonia. *Electrochim. Acta* **56**, 8085–8093 (2011).
130. Lee, S. A., Lee, M. G. & Jang, H. W. Catalysts for electrochemical ammonia oxidation: trend, challenge, and promise. *Sci. China Mater.* **65**, 3334–3352 (2022).
131. Novell-Leruth, G., Valcárcel, A., Pérez-Ramírez, J. & Ricart, J. M. Ammonia dehydrogenation over platinum-group metal surfaces. Structure, stability, and reactivity of adsorbed NH_x species. *J. Phys. Chem. C* **111**, 860–868 (2007).
132. Daramola, D. A. & Botte, G. G. Theoretical study of ammonia oxidation on platinum clusters—adsorption of ammonia and water fragments. *Comput. Theor. Chem.* **989**, 7–17 (2012).
133. Katsounaros, I. et al. On the mechanism of the electrochemical conversion of ammonia to dinitrogen on Pt(100) in alkaline environment. *J. Catal.* **359**, 82–91 (2018).
134. Rouwenhorst, K. H. R., Van der Ham, A. G. J., Mul, G. & Kersten, S. R. A. Islanded ammonia power systems: technology review & conceptual process design. *Renew. Sustain. Energy Rev.* **114**, 109339 (2019).
135. Cai, A. & Rozario, Z. Direct ammonia fuel cells: a general overview, current technologies and future directions. *Johns. Matthey Technol. Rev.* **66**, 479–489 (2022).
136. Halseid, R., Vie, P. J. S. & Tunold, R. Effect of ammonia on the performance of polymer electrolyte membrane fuel cells. *J. Power Sources* **154**, 343–350 (2006).
137. Li, J. et al. Ammonia and hydrogen blending effects on combustion stabilities in optical SI engines. *Energy Convers. Manage.* **280**, 116827 (2023).
138. Jeerh, G., Zhang, M. & Tao, S. Recent progress in ammonia fuel cells and their potential applications. *J. Mater. Chem. A* **9**, 727–752 (2021).
139. Yang, J. et al. A stability study of Ni/yttria-stabilized zirconia anode for direct ammonia solid oxide fuel cells. *ACS Appl. Mater. Interfaces* **7**, 28701–28707 (2015).
140. Akimoto, W. et al. Ni–Fe/Sm-doped CeO_2 anode for ammonia-fueled solid oxide fuel cells. *Solid State Ion.* **256**, 1–4 (2014).
141. Song, Y. et al. Infiltrated NiCo alloy nanoparticle decorated perovskite oxide: a highly active, stable, and antisintering anode for direct-ammonia solid oxide fuel cells. *Small* **16**, 2001859 (2020).
142. Meng, G., Jiang, C., Ma, J., Ma, Q. & Liu, X. Comparative study on the performance of a SDC-based SOFC fueled by ammonia and hydrogen. *J. Power Sources* **173**, 189–193 (2007).
143. Hashinokuchi, M., Zhang, M., Doi, T. & Inaba, M. Enhancement of anode activity and stability by Cr addition at Ni/Sm-doped CeO_2 cermet anodes in NH_3-fueled solid oxide fuel cells. *Solid State Ion.* **319**, 180–185 (2018).
144. Wan, Z., Tao, Y., Shao, J., Zhang, Y. & You, H. Ammonia as an effective hydrogen carrier and a clean fuel for solid oxide fuel cells. *Energy Convers. Manage.* **228**, 113729 (2021).
145. Zhu, L. et al. Ammonia-fed reversible protonic ceramic fuel cells with Ru-based catalyst. *Commun. Chem.* **4**, 121 (2021).
146. Müller, M., Pfeifer, M., Holtz, D. & Müller, K. Comparison of green ammonia and green hydrogen pathways in terms of energy efficiency. *Fuel* **357**, 129843 (2024).
147. Wen, D. & Aziz, M. Techno-economic analyses of power-to-ammonia-to-power and biomass-to-ammonia-to-power pathways for carbon neutrality scenario. *Appl. Energy* **319**, 119272 (2022).
148. Lin, Z., Li, D. & Zou, Y. Energy efficiency of lithium-ion batteries: influential factors and long-term degradation. *J. Energy Storage* **74**, 109386 (2023).
149. Xie, Q. et al. Non-thermal atmospheric plasma synthesis of ammonia in a DBD reactor packed with various catalysts. *J. Phys. D* **53**, 064002 (2020).
150. Li, S., van Raak, T. & Gallucci, F. Investigating the operation parameters for ammonia synthesis in dielectric barrier discharge reactors. *J. Phys. D* **53**, 014008 (2020).
151. Hu, X., Zhu, X., Wu, X., Cai, Y. & Tu, X. Plasma-enhanced NH_3 synthesis over activated carbon-based catalysts: effect of active metal phase. *Plasma Process. Polym.* **17**, 2000072 (2020).
152. Wang, Y. et al. Plasma-enhanced catalytic synthesis of ammonia over a Ni/Al_2O_3 catalyst at near-room temperature: insights into the importance of the catalyst surface on the reaction mechanism. *ACS Catal.* **9**, 10780–10793 (2019).
153. Liu, Y. et al. Synergistic effect of Co–Ni bimetal on plasma catalytic ammonia synthesis. *Plasma Chem. Plasma Process.* **42**, 267–282 (2022).
154. Zhu, X. et al. Plasma-catalytic synthesis of ammonia over Ru-based catalysts: insights into the support effect. *J. Energy Inst.* **102**, 240–246 (2022).

Acknowledgements
X.F. acknowledges support from the National University of Singapore start-up grant. P.X. acknowledges funding from National Key Research and Development Program of China (2023YFA1508103) and the National Natural Science Foundation of China (22278365). X.T. acknowledges funding from the European Union's Horizon Europe Research and Innovation Programme under grant agreement no. 101083905 and the UK Research and Innovation Horizon Europe Guarantee Fund (no. 10055396).

Author contributions
Introduction (X.F. and Z.W.); Ammonia as an energy carrier (X.F. and Z.W.); Ammonia synthesis under mild conditions (X.F., X.T., Z.W. and Y.W.); Ammonia decomposition for hydrogen production (P.X., K.W. and X.F.); Ammonia fuel cells (P.X., B.H. and X.F.); Overview of the review (X.F., P.X. and X.T.). All authors discussed and edited the full manuscript.

Competing interests
The authors declare no competing interests.

Additional information
Supplementary information The online version contains supplementary material available at https://doi.org/10.1038/s44359-025-00102-9.

Peer review information *Nature Reviews Clean Technology* thanks Hoang-Long Du, Kwiyong Kim, Chenglin Yan and the other, anonymous, reviewer(s) for their contribution to the peer review of this work.